Multi-approach gravity field models from Swarm GPS data

Signal and error in the Swarm models up to 2020-12-31

Delft University of Technology (TU Delft)
Astronomical Institute of the University of Bern (AIUB)
Astronomical Institute Ondřejov (ASU)
Institute of Geodesy Graz (IfG)
Ohio State University (OSU)

Version 1.0
2021-03-13

Prepared and checked by	Approved by
João Encarnação	Pieter Visser
Work Package Manager	Project Manager

©Delft University of Technology, The Netherlands, 2021. Proprietary and intellectual rights of Delft University of Technology, The Netherlands are involved in the subject-matter of this material and all manufacturing, reproduction, use, disclosure, and sales rights pertaining to such subject-matter are expressly reserved. This material is submitted for a specific purpose as agreed in writing, and the recipient by accepting this material agrees that this material will not be used, copied, or reproduced in whole or in part nor its contents (or any part thereof) revealed in any manner or to any third party, except own staff, to meet the purpose for which it was submitted and subject to the terms of the written agreement.

Contents

List of Figures

The use and/or disclosure, etc. of the contents of this document (or any part thereof) is subject to the restrictions referenced on the front page.

List of Tables

The use and/or disclosure, etc. of the contents of this document (or any part thereof) is subject to the restrictions referenced on the front page.

1 Version history

Version 1,2021-03-13

- Validation of combined models version 09, from start of mission until 2020-12-31.

2 Introduction

We report some statistics of the individual and combined GFMs produced on the context of the *Multi-approach gravity field models from Swarm GPS data* project. The approach for combining individual gravity field solutions, i.e. those produced by the various partners mentioned in Section 3, is described in Section 4.1. The procedure and assumption used to derive the statistics is described in Section 4.2. Finally, the results are presented in Section 5.

This report does not intend to draw conclusions regarding the presented statistics, it is merely a descriptive document of the signal and error in the individual and combined Swarm GFMs. For this reason, the text in Section 5 is restricted to clarifying the quantities shown in the plots.

3 Source data

The individual gravity field solutions are produced by the institutes listed in Table 1.

Additional details about the different gravity field approaches can be found in (Teixeira da Encarnação and Visser, 2017).

The version of the individual GFMs is listed in Table 2.

The version numbers listed in Table 2 are relevant within the project and are reported so that it is possible to trace back the results presented in Section 5. Particular to the combined models, version 09 relates to the chosen combination strategy, as concluded from Teixeira da Encarnação and Visser (2019).

The use and/or disclosure, etc. of the contents of this document (or any part thereof) is subject to the restrictions referenced on the front page.

Table 1 – Overview of the gravity field estimation approaches

Inst.	Approach	Reference
AIUB	Celestial Mechanics Approach (Beutler et al., 2010)	Jäggi et al. (2016)
ASU	Decorrelated Acceleration Approach (Bezděk et al., 2014; Bezděk et al., 2016)	Bezděk et al. (2016)
IfG	Short-Arcs Approach (Mayer-Gürr, 2006)	Zehentner and Mayer-Gürr (2016)
OSU	Improved Energy Balance Approach (Shang et al., 2015)	Guo et al. (2015)

Gravity Field Model	version	Kinematic Orbit
AIUB	01	AIUB
ASU	02	IfG
IfG	03 – 06	IfG
OSU	02	AIUB
combined	09	N/A

Table 2 – Versions of the GFMs, and the KOs used in their estimation, relevant to this report.

4 Methodology

4.1 Combination

The combination of the models is conducted at the level of the solutions considering weights derived from Variance Component Estimation (VCE). As demonstrated in Teixeira da Encarnação and Visser (2019), the combination at the level of Normal Equation (NEQ) disagreed more with GRACE/GRACE-FO, as a result of the vastly different amplitudes of formal errors.

The combination considers the complete degree range (degrees 2 to 40) but the VCE weights are derived from degrees 2-20. This approach addresses the very high errors above degree 20, which would otherwise drive the value of the weights.

It is feasible to determine the VCE weights because there are two time-series based on AIUB orbits (i.e. AIUB and OSU) and two time-series based on IfG orbits (i.e. IfG and ASU). Therefore the impact of the KOs on the solutions and on the VCE weights is balanced.

4.2 Validation

The validation is done by comparing the individual and combined solutions to a model estimated from the Release 6 (RL06) GRACE/GRACE-FO GFMs produced at Center for Space Research (CSR), considering all solutions available at the this document is produced. This models fits a degree 1 polynomial and a yearly, semi-yearly, S2, K1 and K2 periods to the GRACE/GRACE-FO time series; the time series produced on the basis of the parameters resulting from this regression are referred to as *GRACE/GRACE-FO climatological model*.

The $C_{2,0}$ coefficient in all solutions has been replaced by the weekly time series provided by Goddard Space Flight Center (GSFC) (Loomis, Rachlin and Luthcke, 2019).

All solutions undergo a 750km radius spherical cap Gaussian filtering, unless otherwise noted, to clearly show the geophysical signal contained in the Swarm solutions. The GRACE and GOCE Gravity Model 05 (GGM05G) (Bettadpur et al., 2015) static GFM is subtracted from all models in order to isolate the time-variable component of Earth's gravity field. We chose to show the gravity field in terms of EWH, except for the statistics related to the correlation

The use and/or disclosure, etc. of the contents of this document (or any part thereof) is subject to the restrictions referenced on the front page.

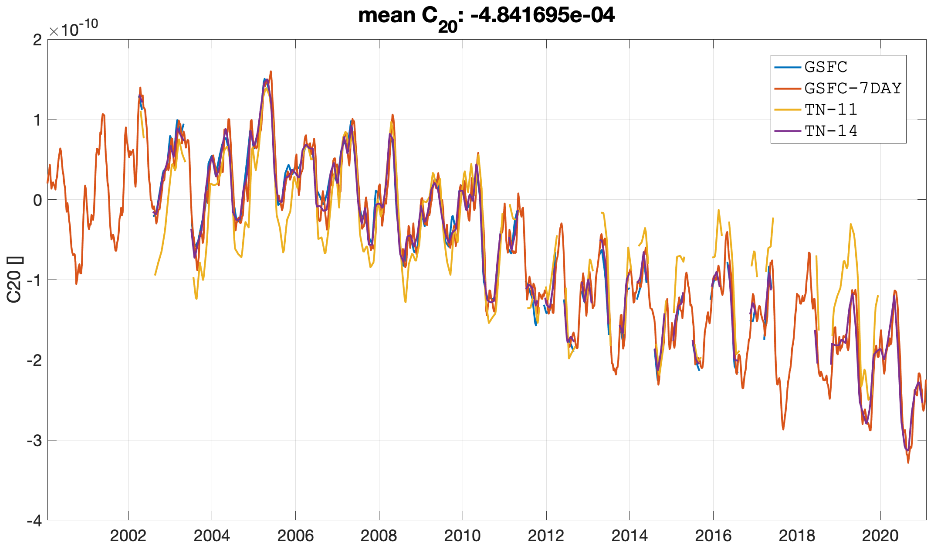

Figure 1 – Monthly (GSFC) and weekly (GSFC-7DAY) versions of the time series of SLR-derived C_{20} from Loomis, Rachlin and Luthcke (2019), compared to Cheng and Ries (2018) (TN-11) and Loomis and Rachlin (2020) (TN-14).

coefficient, which are non-dimensional as usual. The GRACE/GRACE-FO gravity field time series is linearly interpolated to the mid-month epoch of the Swarm solutions. The GRACE/GRACE-FO climatological model is evaluated at the same time domain. The analysis spans 2016-01-01 until 2020-12-31.

Some analyses are restricted to either the land or ocean areas. In those cases, the land or ocean mask is applied in the spatial domain and a Spherical Harmonic (SH) analysis is done on the masked grid. The ocean mask excludes the coastal ocean areas that are roughly 1000km or less from land areas, as shown in Figure 2, while the land mask has no buffer zone.

In Section 5.4, the geophysical signal represented by the Swarm solutions is evaluated on the basis of the time series of average EWH over restricted geographical locations, shown in Figure 3.

Each averaging is done over the corresponding spatial truncation of an equiangular grid representation of the SH coefficients. The locations shown in Sections 5.4.1 to 5.4.18 are related to the largest hydrological basins and polar regions with the highest signal variability observed by GRACE/GRACE-FO. Note that there is no effort to meticulously consider or implement proper leakage reduction methods, e.g. by Guo, Duan and Shum (2010). We perform a parametric regression on all time series considering a constant and drift terms, along with annual and semi-annual sine and co-sine terms to improve the robustness. We plot the linear part of this regression, in order to quantify the accuracy of Swarm-derived climatological trends. The time series are plotted along with tables presenting some statistics. The values of the constant and linear terms for the Swarm and GRACE/GRACE-FO solutions (column 1) are show in terms of EWH (columns 2 and 4). Additionally, the difference of these parameters between the Swarm and GRACE/GRACE-FO solutions relative to the GRACE/GRACE-FO climatological model is listed in columns 3 and 5 (the values for the latter data set in these columns is zero). Finally, the correlation coefficients is presented in the last column (the value for GRACE/GRACE-FO climatological model is 1). The constant term is the average basin storage over the relevant data period.

The use and/or disclosure, etc. of the contents of this document (or any part thereof) is subject to the restrictions referenced on the front page.

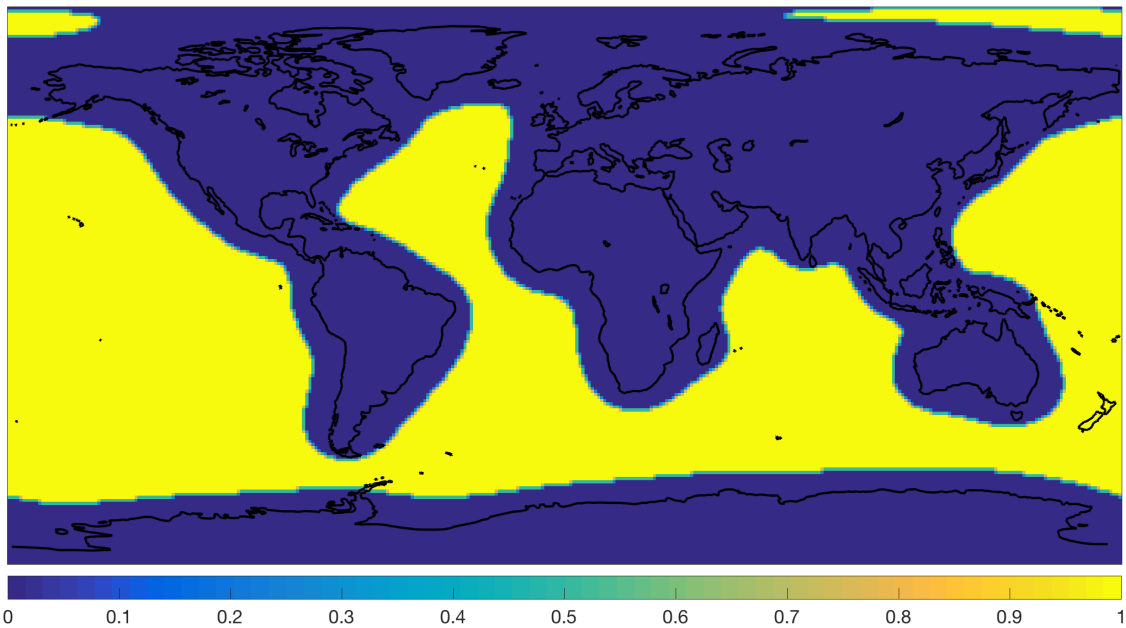

Figure 2 – Deep ocean mask.

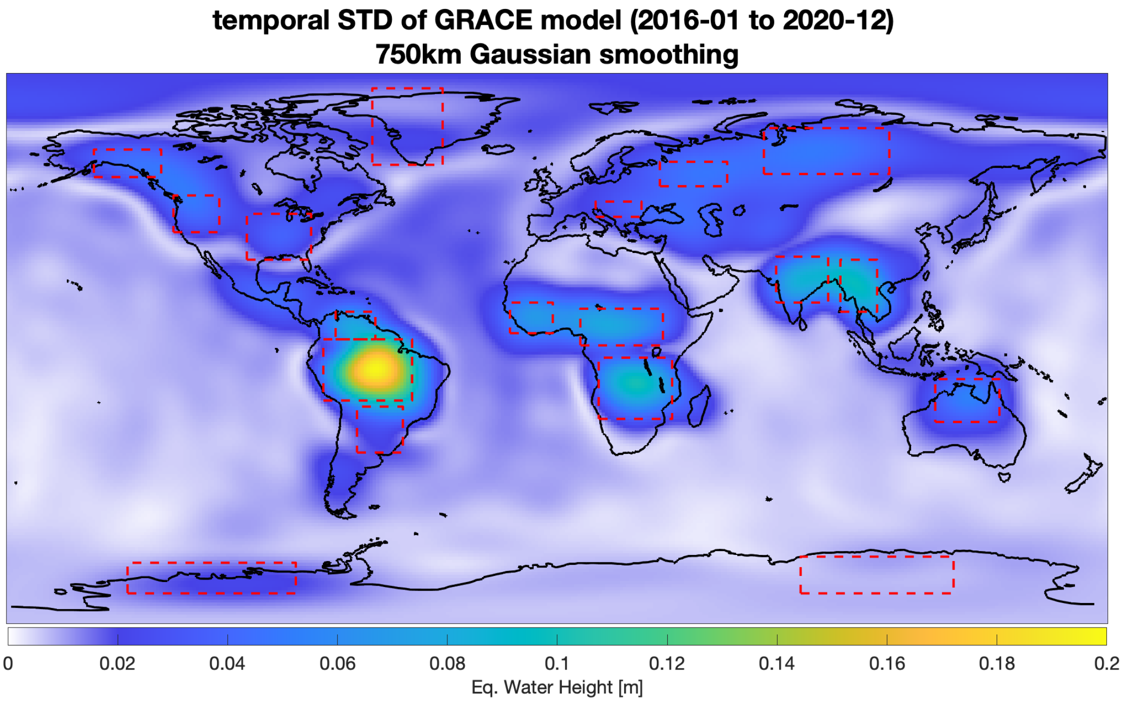

Figure 3 – Temporal variability of the GRACE/GRACE-FO climatological model, including the boundaries of the regions analysed in Section 5.4.1 to Section 5.4.18.

The use and/or disclosure, etc. of the contents of this document (or any part thereof) is subject to the restrictions referenced on the front page.

5 Results

5.1 Spatial analysis

5.1.1 Degree-mean RMS difference

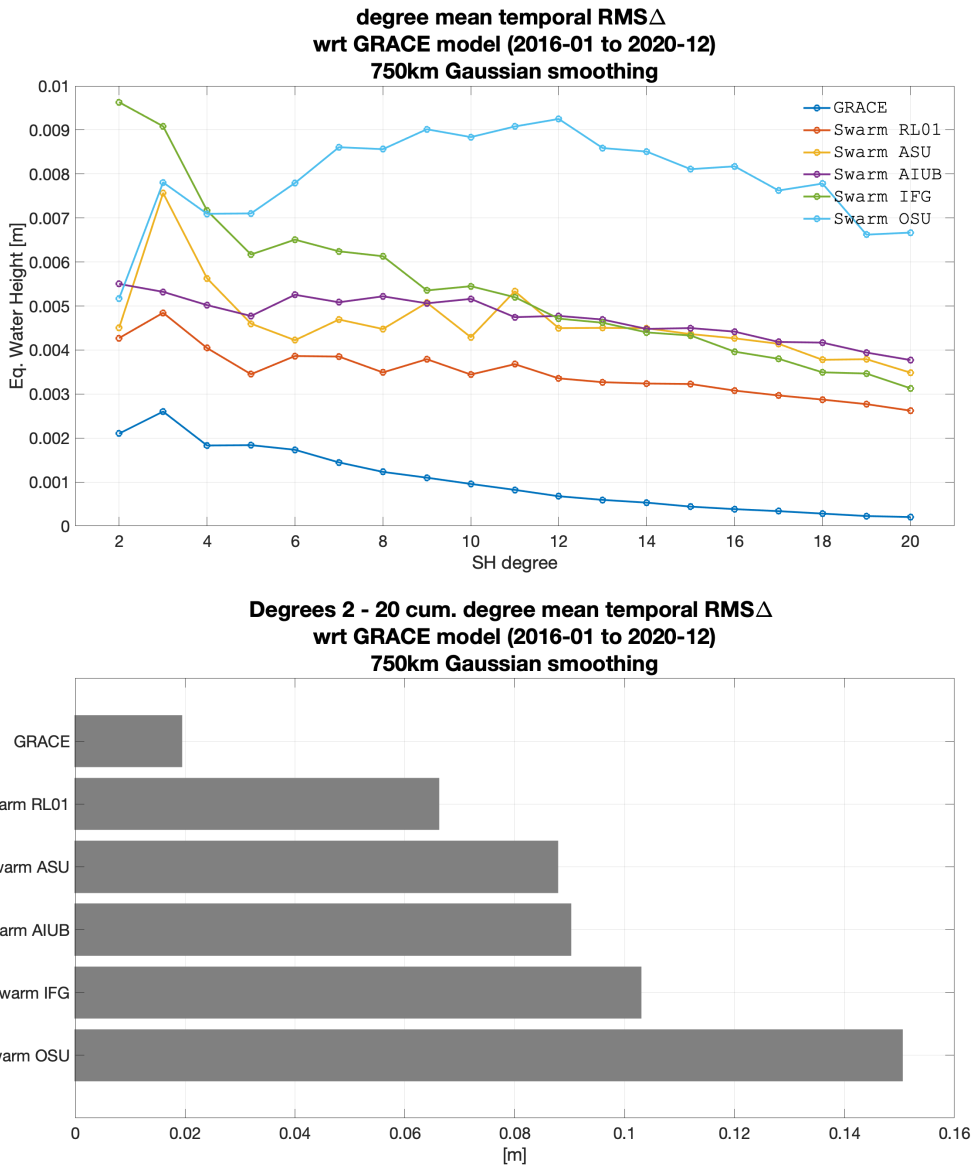

Figure 4 – Per-degree mean of the RMS difference (top) and cumulative degree-mean temporal RMS difference (bottom) between the Swarm GFMs and GRACE-based prediction, considering 750km Gaussian smoothing. This is (an estimate of) the average per-degree quality of the various Swarm solutions in the spectral domain (top) and globally (bottom) . The degree amplitudes remain relatively constant with increasing degree, instead of growing in terms of EWH, as the result of the smoothing.

5.1.2 Cumulative degree amplitude difference over land

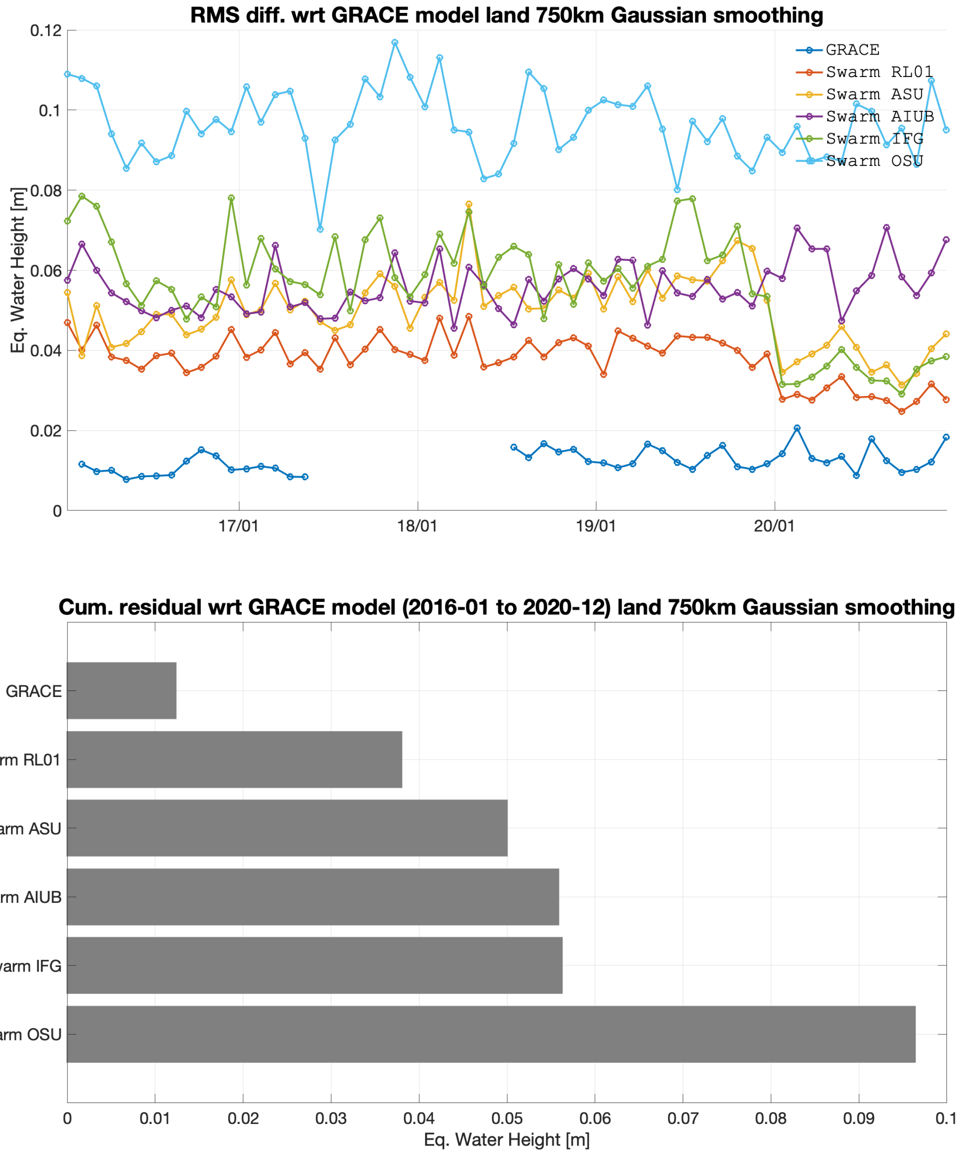

Figure 5 – Epoch-wise cumulative spatial RMS (top) and its global average (bottom) of the difference between Swarm GFMs and GRACE-based prediction, over land areas, considering 750km Gaussian smoothing. This is (an estimate of) the evolution of the ability of the various Swarm solutions to predict land mass transport processes over time (top) and its global sum (bottom).

The use and/or disclosure, etc. of the contents of this document (or any part thereof) is subject to the restrictions referenced on the front page.

5.1.3 Cumulative degree amplitude difference over oceans

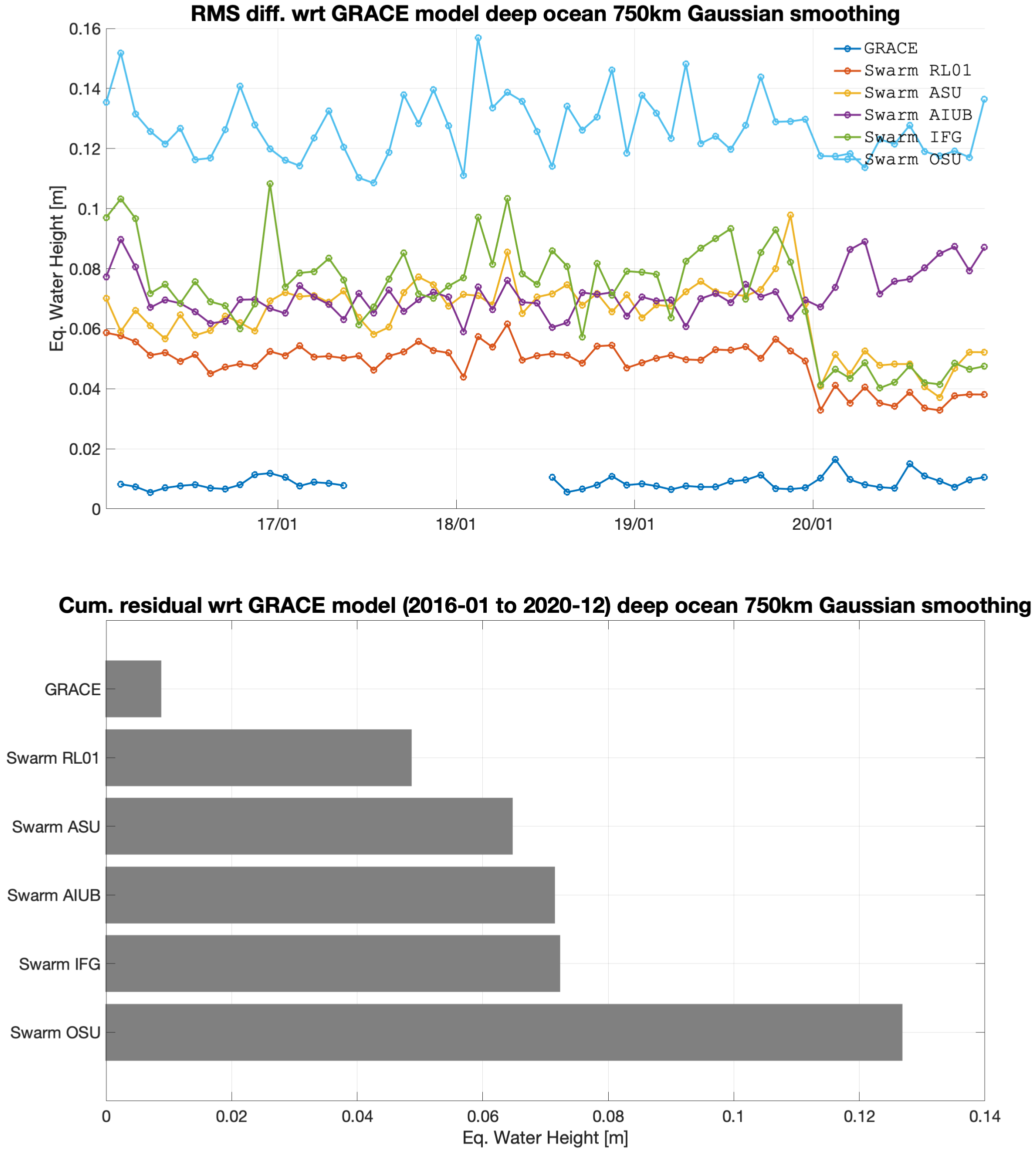

Figure 6 – Epoch-wise cumulative spatial RMS (top) and its global sum (bottom) of the difference between Swarm GFMs and GRACE-based prediction, over ocean areas, considering 750km Gaussian smoothing. This is the epoch-wise quality of the Swarm GFMs, and reported in the header of the combined GFMs files.

5.2 Temporal analysis

5.2.1 Per-degree mean correlation coefficient over land

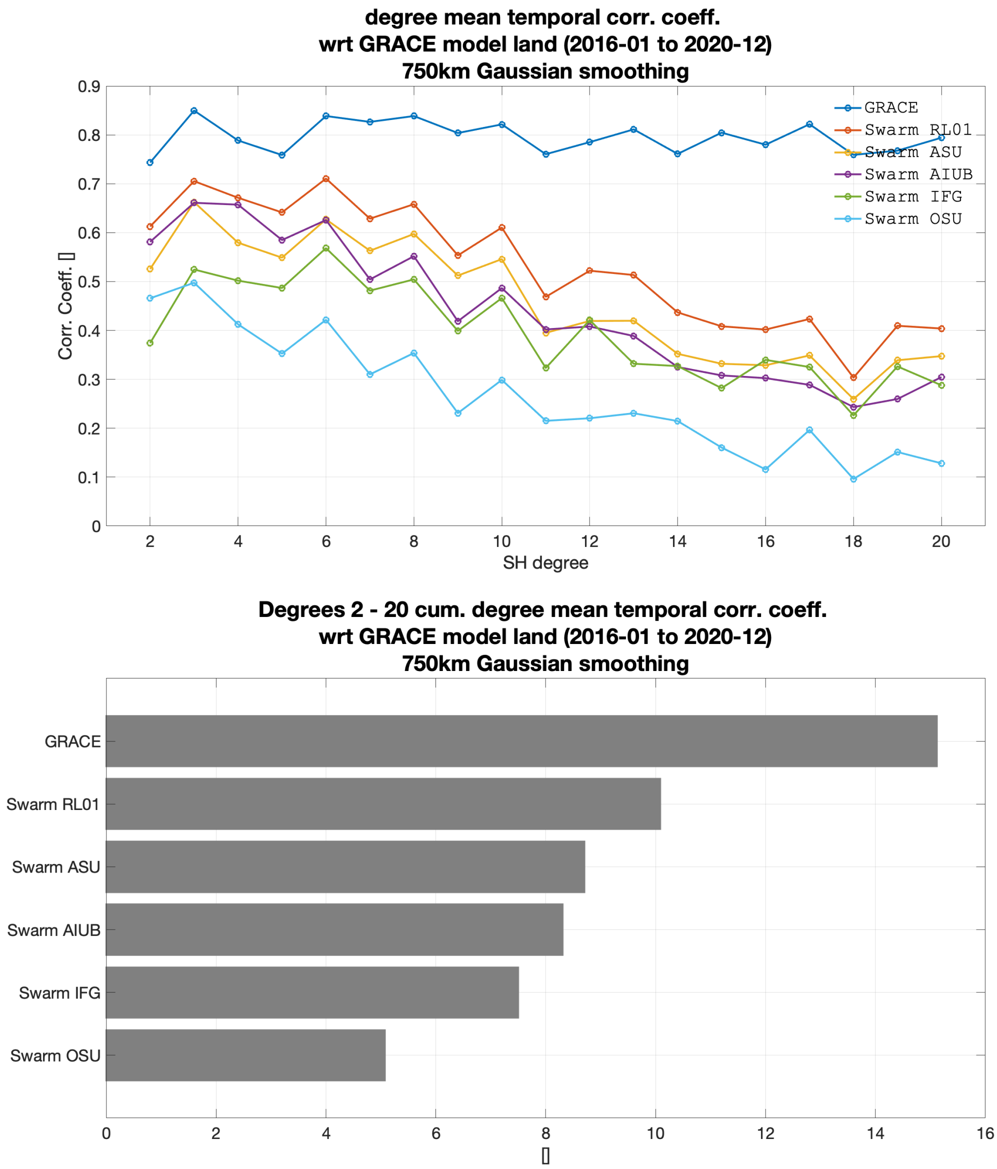

Figure 7 – Per-degree mean (top) and its overall cumulative (bottom) of the correlation coefficient between Swarm GFMs and GRACE-based prediction, over land areas, considering 750km Gaussian smoothing. The temporal correlation at every Stokes coefficient is computed and the average over each degree is plotted at the top. It illustrates how well the temporal variations of the Swarm models agree with what is predicted from the GRACE/GRACE-FO climatological model.

The use and/or disclosure, etc. of the contents of this document (or any part thereof) is subject to the restrictions referenced on the front page.

5.2.2 Per-degree mean correlation coefficient over oceans

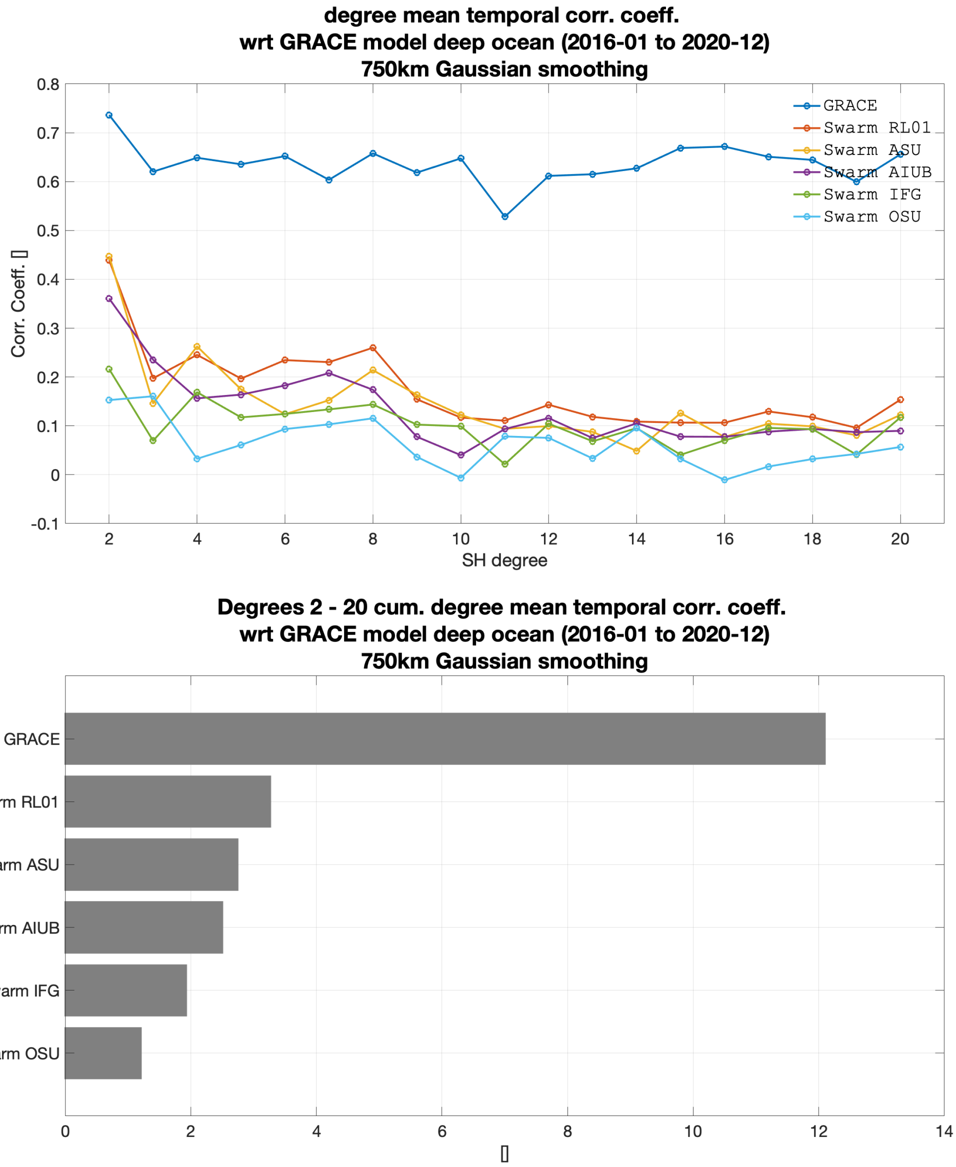

Figure 8 – Per-degree mean (top) and its overall cumulative (bottom) of the correlation coefficient between Swarm GFMs and GRACE-based prediction, over ocean areas, considering 750km Gaussian smoothing. It illustrates that the Swarm models agree poorly with the mass variations over the ocean as predicted by the GRACE/GRACE-FO climatological model.

The use and/or disclosure, etc. of the contents of this document (or any part thereof) is subject to the restrictions referenced on the front page.

5.2.3 Global unsmoothed per-degree mean correlation coefficient

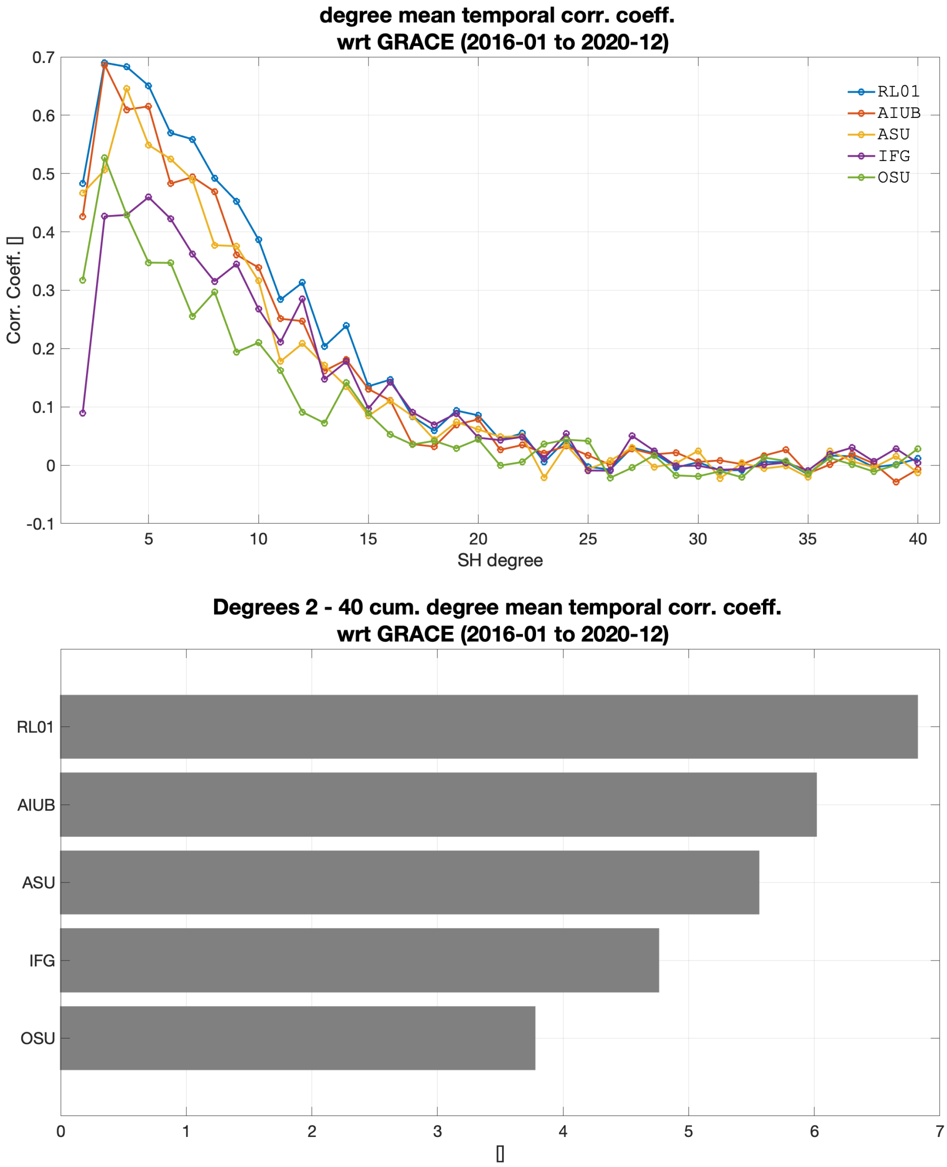

Figure 9 – Per-degree mean (top) and its overall cumulative (bottom) of the correlation coefficient between Swarm and GRACE/GRACE-FO GFMs (not the GRACE/GRACE-FO climatological model), globally and with no smoothing. It illustrates that the Swarm models fail to represent the same temporal variations as GRACE/GRACE-FO above degree 15-20.

The use and/or disclosure, etc. of the contents of this document (or any part thereof) is subject to the restrictions referenced on the front page.

5.2.4 Triangular plots of the RMS differences

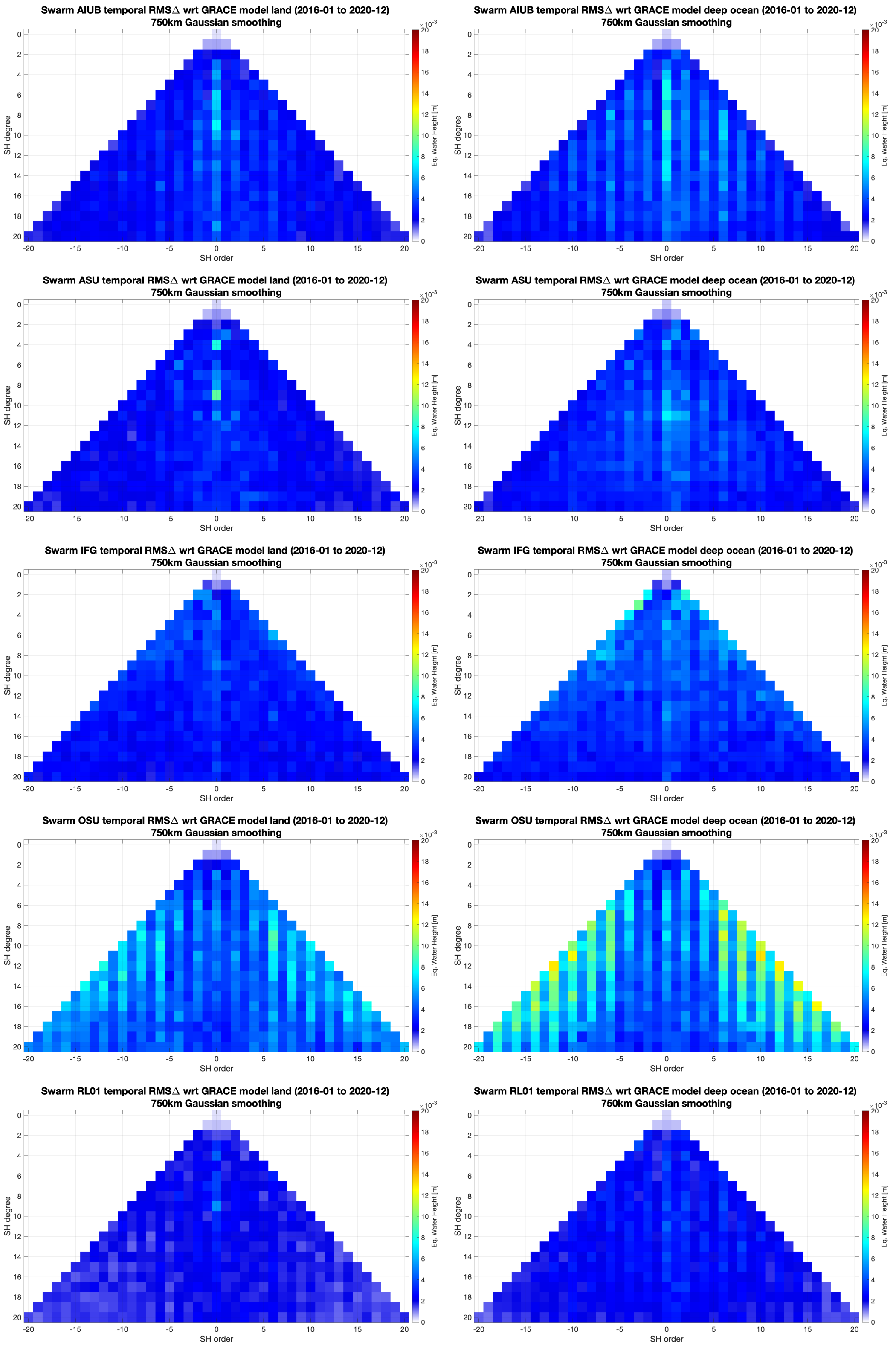

Figure 10 – Per-coefficient RMS difference between Swarm GFMs and GRACE-based prediction considering 750km Gaussian smoothing, over land (left column) and ocean (right column) areas, for AIUB, ASU, IfG, OSU and combined solutions (respectively from top to bottom).

The use and/or disclosure, etc. of the contents of this document (or any part thereof) is subject to the restrictions referenced on the front page.

5.3 Monthly models

5.3.1 Monthly degree-RMS

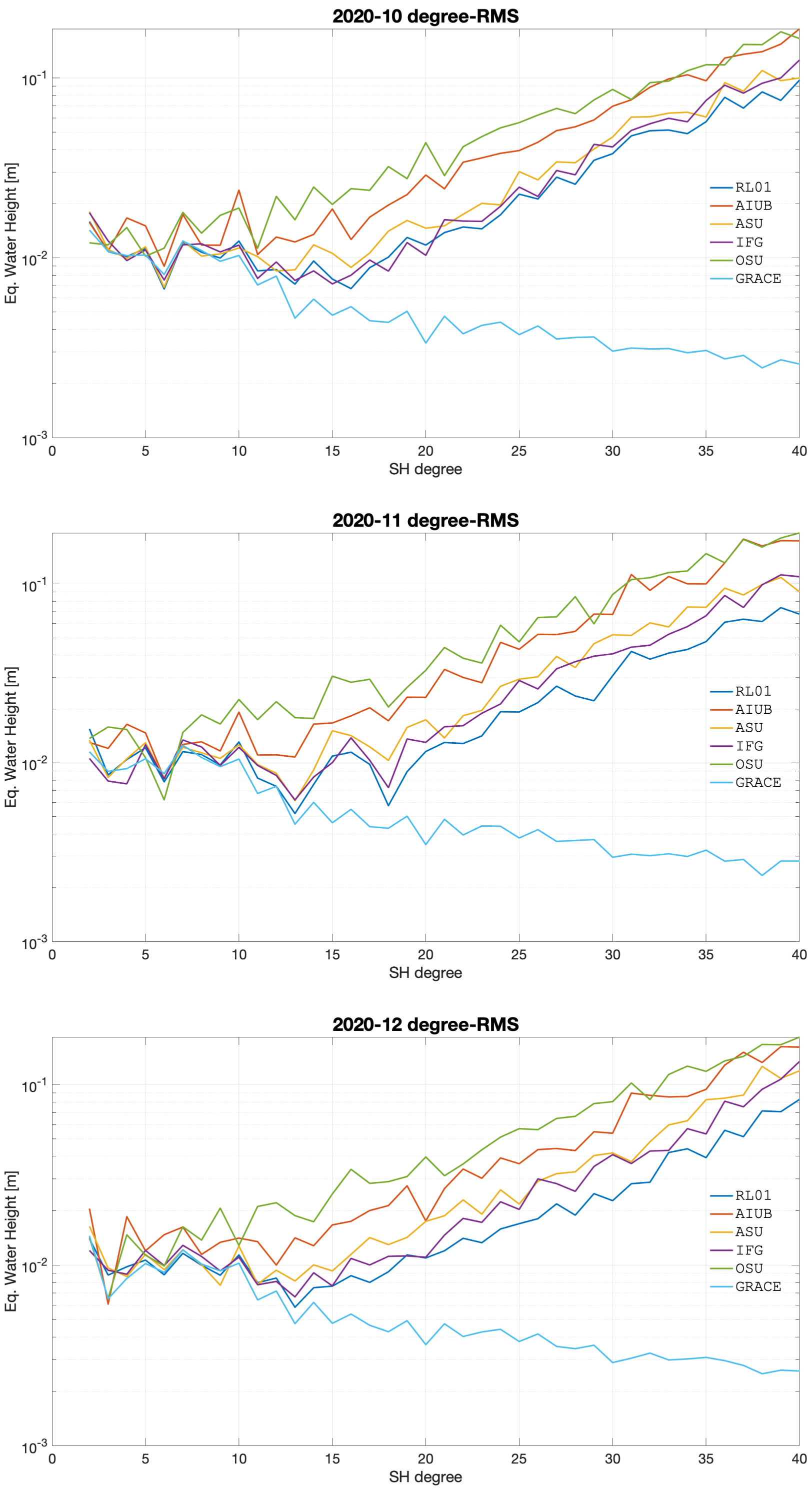

Figure 11 – Monthly degree-RMS for the 3 most recent months, all individual and combined Swarm solutions, as well as GRACE/GRACE-FO (no smoothing).

5.4 Time series of storage catchments

5.4.1 Amazon basin

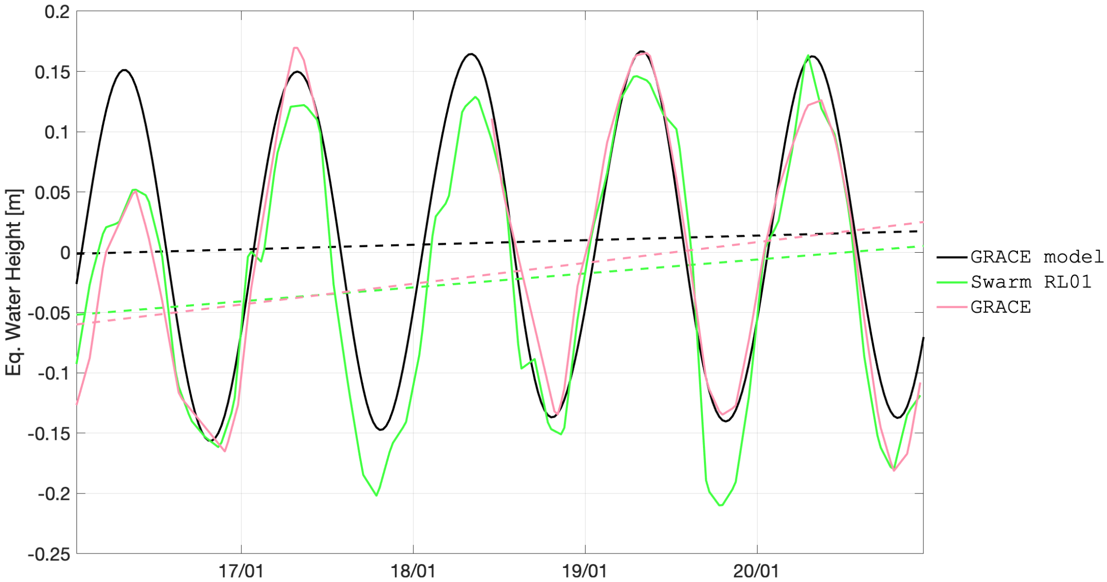

Figure 12 – Time series of EWH for the Amazon basin (latitude -17 to 3 degrees, longitude -76 to -47 degrees).

solution	constant term [cm]	constant term Δ [cm]	linear term [cm/year]	linear term Δ [cm/year]	corr. coeff. [ ]
GRACE MODEL	0.81	0.00	0.38	0.00	1.00
Swarm RL01	-2.31	-3.12	1.16	0.77	0.95
GRACE	-0.04	-0.85	1.72	1.34	0.92

Table 3 – Statistics of the agreement between GRACE/GRACE-FO and Swarm time series relative to the GRACE/GRACE-FO climatological model for the Amazon basin.

5.4.2 Orinoco basin

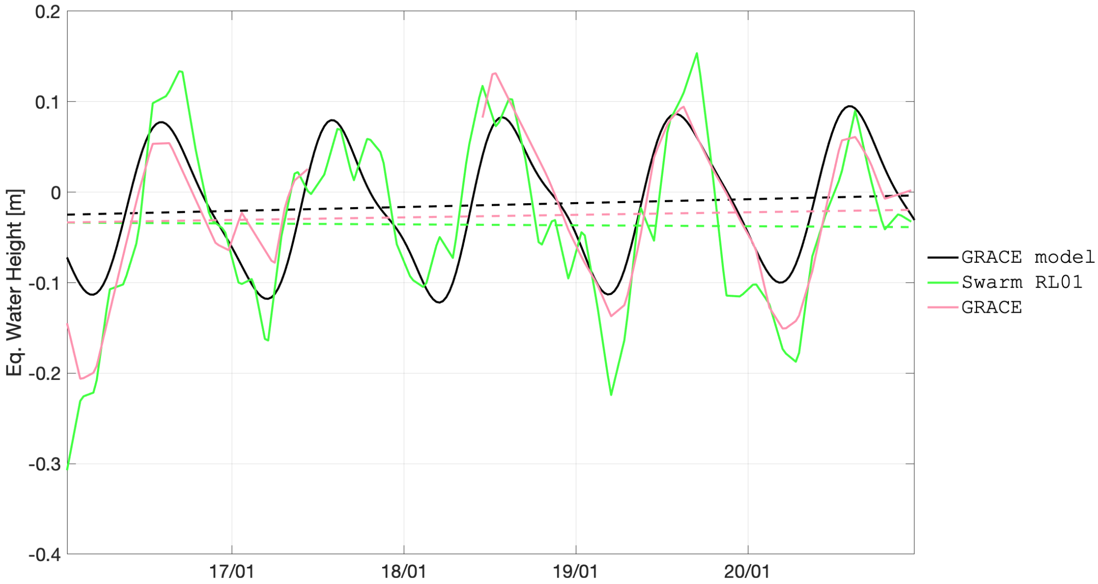

Figure 13 – Time series of EWH for the Orinoco basin (latitude -3 to 12 degrees, longitude -72 to -59 degrees).

solution	constant term [cm]	constant term Δ [cm]	linear term [cm/year]	linear term Δ [cm/year]	corr. coeff. [ ]
GRACE MODEL	-1.43	0.00	0.43	0.00	1.00
Swarm RL01	-3.67	-2.24	-0.10	-0.53	0.82
GRACE	-2.72	-1.30	0.28	-0.15	0.89

Table 4 – Statistics of the agreement between GRACE/GRACE-FO and Swarm time series relative to the GRACE/GRACE-FO climatological model for the Orinoco basin.

5.4.3 La Plata basin

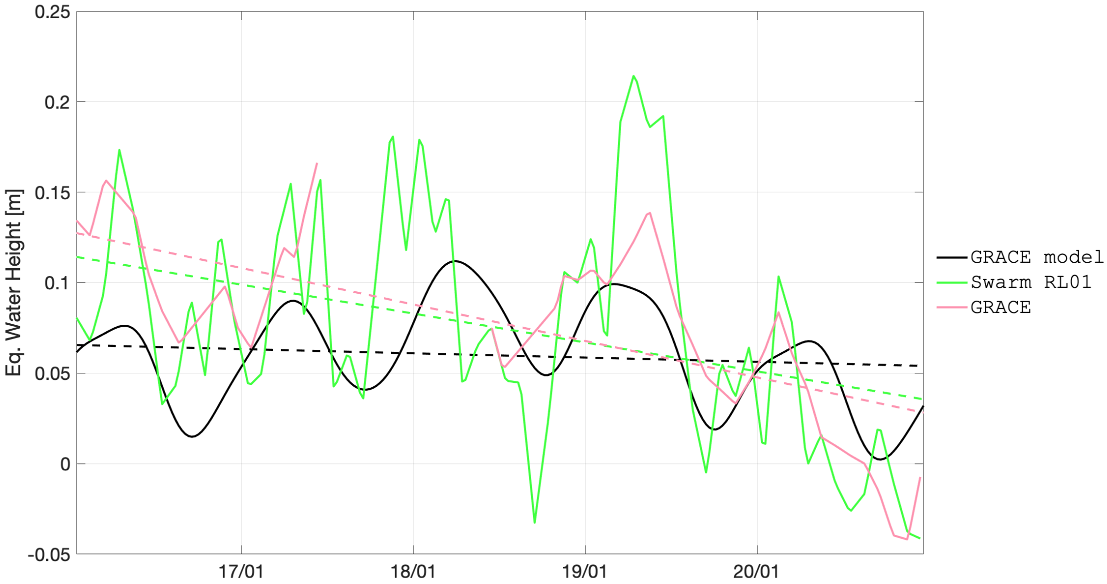

Figure 14 – Time series of EWH for the La Plata basin (latitude -34 to -19 degrees, longitude -65 to -50 degrees).

solution	constant term [cm]	constant term Δ [cm]	linear term [cm/year]	linear term Δ [cm/year]	corr. coeff. [ ]
GRACE MODEL	5.98	0.00	-0.23	0.00	1.00
Swarm RL01	7.51	1.53	-1.60	-1.36	0.61
GRACE	7.42	1.44	-2.01	-1.78	0.71

Table 5 – Statistics of the agreement between GRACE/GRACE-FO and Swarm time series relative to the GRACE/GRACE-FO climatological model for the La Plata basin.

The use and/or disclosure, etc. of the contents of this document (or any part thereof) is subject to the restrictions referenced on the front page.

5.4.4 Mississippi basin

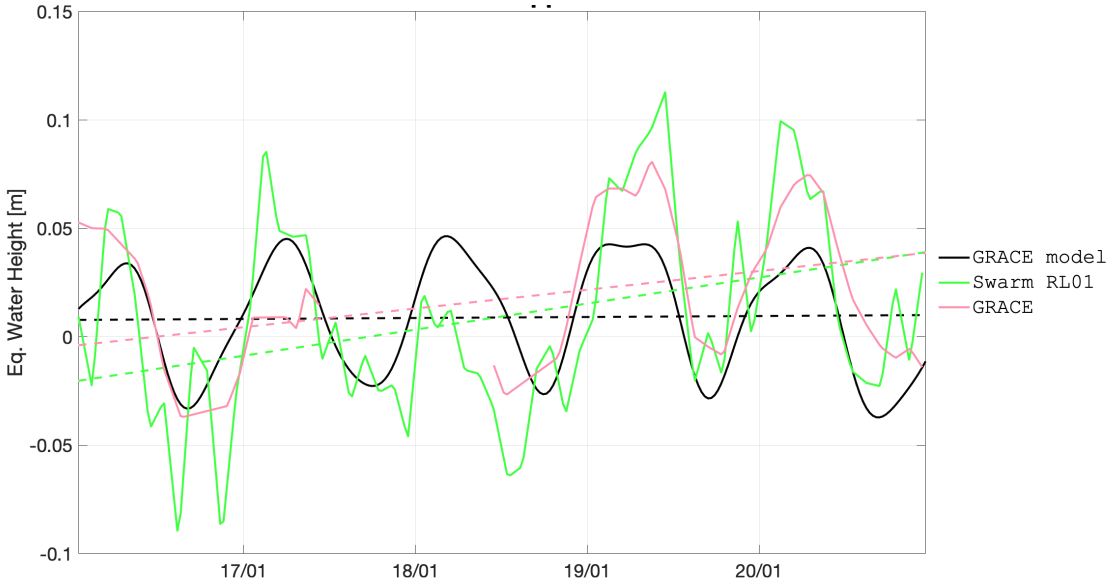

Figure 15 – Time series of EWH for the Mississippi basin (latitude 29 to 44 degrees, longitude -101 to -80 degrees).

solution	constant term [cm]	constant term Δ [cm]	linear term [cm/year]	linear term Δ [cm/year]	corr. coeff. [ ]
GRACE MODEL	0.90	0.00	0.05	0.00	1.00
Swarm RL01	0.95	0.06	1.20	1.16	0.64
GRACE	2.27	1.38	0.86	0.82	0.77

Table 6 – Statistics of the agreement between GRACE/GRACE-FO and Swarm time series relative to the GRACE/GRACE-FO climatological model for the Mississippi basin.

5.4.5 Columbia region

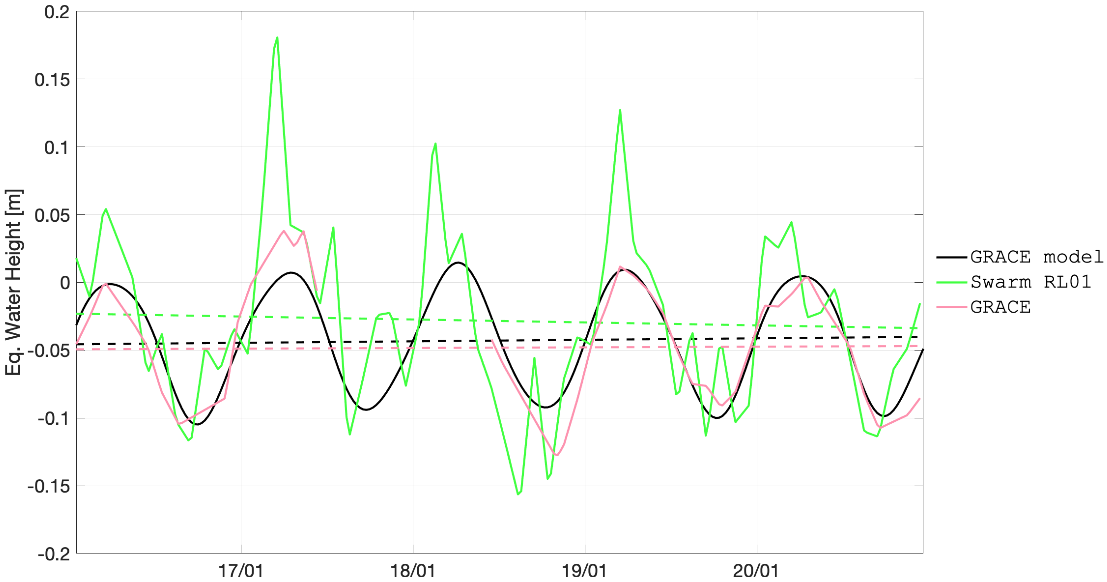

Figure 16 – Time series of EWH for the Columbia region (latitude 38 to 50 degrees, longitude -125 to -110 degrees).

solution	constant term [cm]	constant term Δ [cm]	linear term [cm/year]	linear term Δ [cm/year]	corr. coeff. [ ]
GRACE MODEL	-4.29	0.00	0.11	0.00	1.00
Swarm RL01	-2.80	1.48	-0.22	-0.33	0.77
GRACE	-4.41	-0.12	0.05	-0.06	0.94

Table 7 – Statistics of the agreement between GRACE/GRACE-FO and Swarm time series relative to the GRACE/GRACE-FO climatological model for the Columbia region.

The use and/or disclosure, etc. of the contents of this document (or any part thereof) is subject to the restrictions referenced on the front page.

5.4.6 Alaska

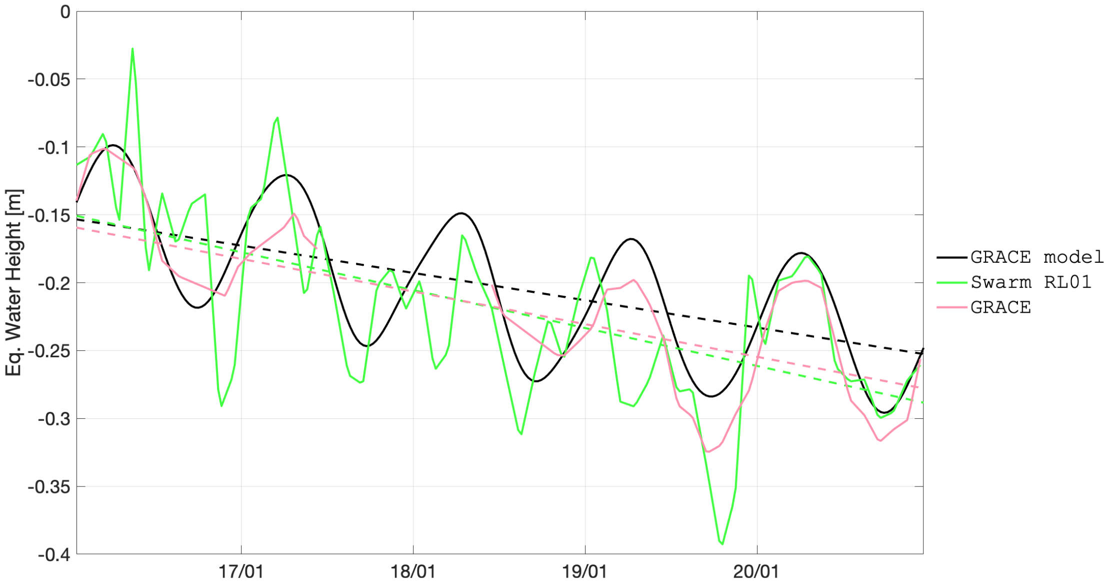

Figure 17 – Time series of EWH for the Alaska (latitude 56 to 65 degrees, longitude -151 to -129 degrees).

solution	constant term [cm]	constant term Δ [cm]	linear term [cm/year]	linear term Δ [cm/year]	corr. coeff. [ ]
GRACE MODEL	-20.29	0.00	-2.01	0.00	1.00
Swarm RL01	-21.92	-1.63	-2.79	-0.78	0.76
GRACE	-22.18	-1.89	-2.40	-0.39	0.95

Table 8 – Statistics of the agreement between GRACE/GRACE-FO and Swarm time series relative to the GRACE/GRACE-FO climatological model for the Alaska.

The use and/or disclosure, etc. of the contents of this document (or any part thereof) is subject to the restrictions referenced on the front page.

5.4.7 Western Greenland region

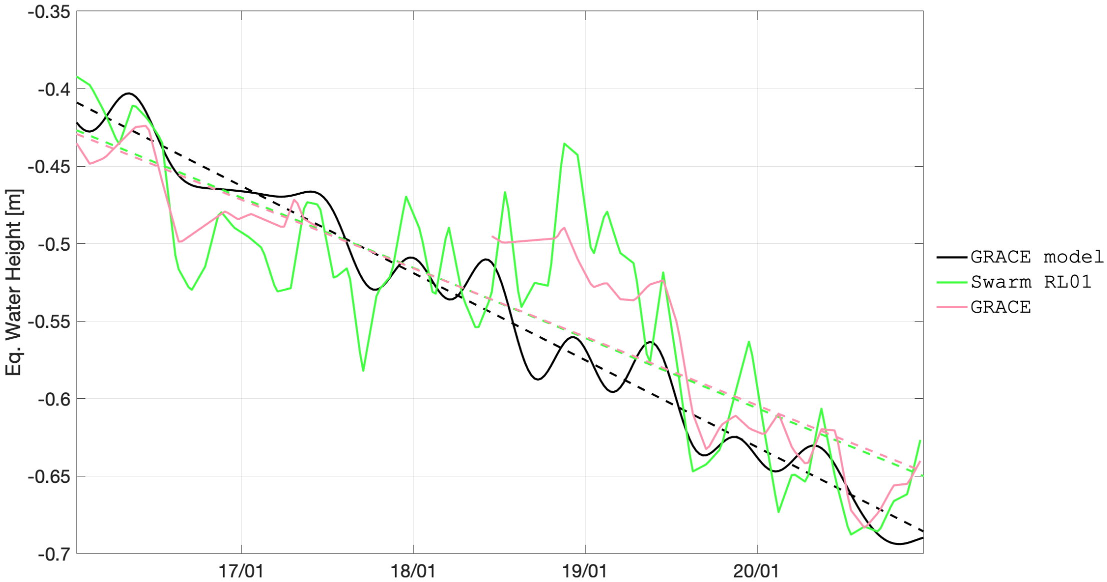

Figure 18 – Time series of EWH for the Western Greenland region (latitude 60 to 85 degrees, longitude -60 to -37 degrees).

solution	constant term [cm]	constant term Δ [cm]	linear term [cm/year]	linear term Δ [cm/year]	corr. coeff. [ ]
GRACE MODEL	-54.71	0.00	-5.62	0.00	1.00
Swarm RL01	-53.81	0.91	-4.53	1.09	0.86
GRACE	-54.76	-0.05	-4.42	1.20	0.93

Table 9 – Statistics of the agreement between GRACE/GRACE-FO and Swarm time series relative to the GRACE/GRACE-FO climatological model for the Western Greenland region.

The use and/or disclosure, etc. of the contents of this document (or any part thereof) is subject to the restrictions referenced on the front page.

5.4.8 Danube basin

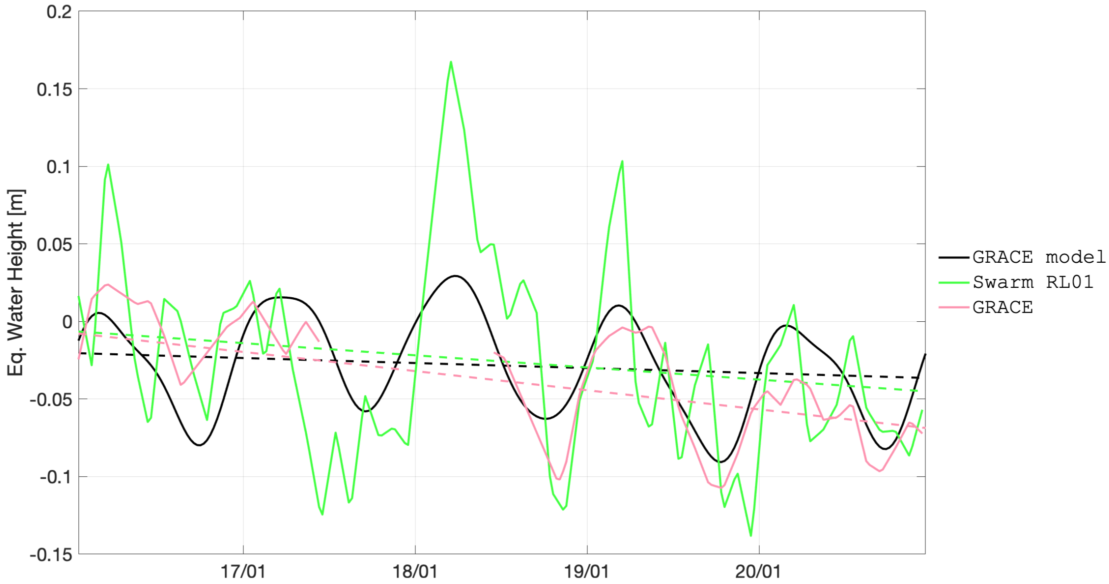

Figure 19 – Time series of EWH for the Danube basin (latitude 43 to 48 degrees, longitude 13 to 28 degrees).

solution	constant term [cm]	constant term Δ [cm]	linear term [cm/year]	linear term Δ [cm/year]	corr. coeff. [ ]
GRACE MODEL	-2.84	0.00	-0.32	0.00	1.00
Swarm RL01	-2.54	0.30	-0.78	-0.46	0.58
GRACE	-3.83	-0.99	-1.23	-0.91	0.74

Table 10 – Statistics of the agreement between GRACE/GRACE-FO and Swarm time series relative to the GRACE/GRACE-FO climatological model for the Danube basin.

5.4.9 Western Sub-Saharan basin

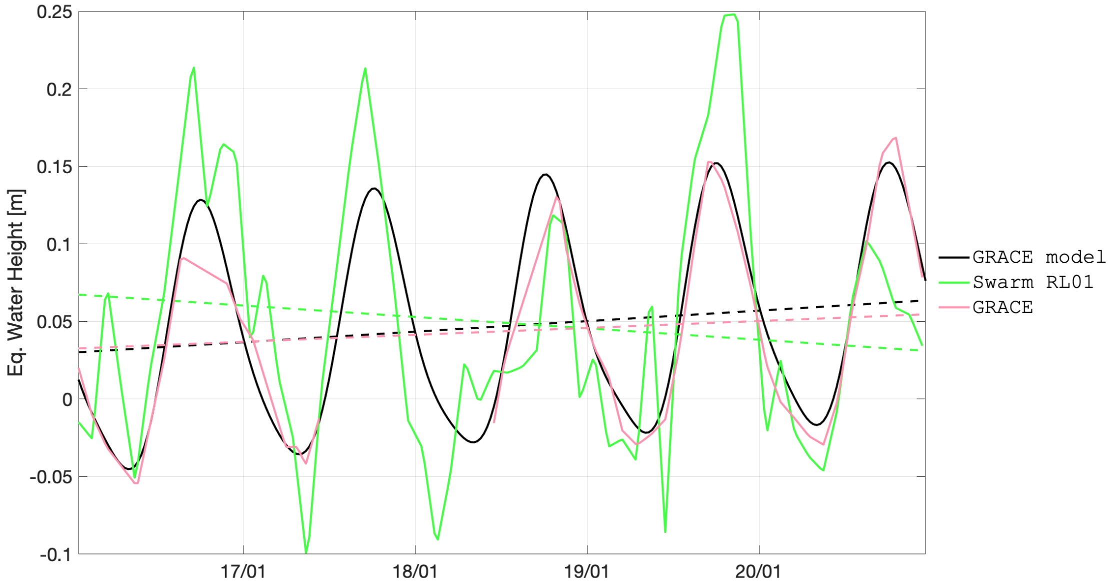

Figure 20 – Time series of EWH for the Western Sub-Saharan basin (latitude 5 to 15 degrees, longitude -15 to -1 degrees).

solution	constant term [cm]	constant term Δ [cm]	linear term [cm/year]	linear term Δ [cm/year]	corr. coeff. [ ]
GRACE MODEL	4.68	0.00	0.68	0.00	1.00
Swarm RL01	4.90	0.22	-0.74	-1.41	0.76
GRACE	3.65	-1.03	0.45	-0.23	0.98

Table 11 – Statistics of the agreement between GRACE/GRACE-FO and Swarm time series relative to the GRACE/GRACE-FO climatological model for the Western Sub-Saharan basin.

The use and/or disclosure, etc. of the contents of this document (or any part thereof) is subject to the restrictions referenced on the front page.

5.4.10 Eastern Sub-Saharan basin

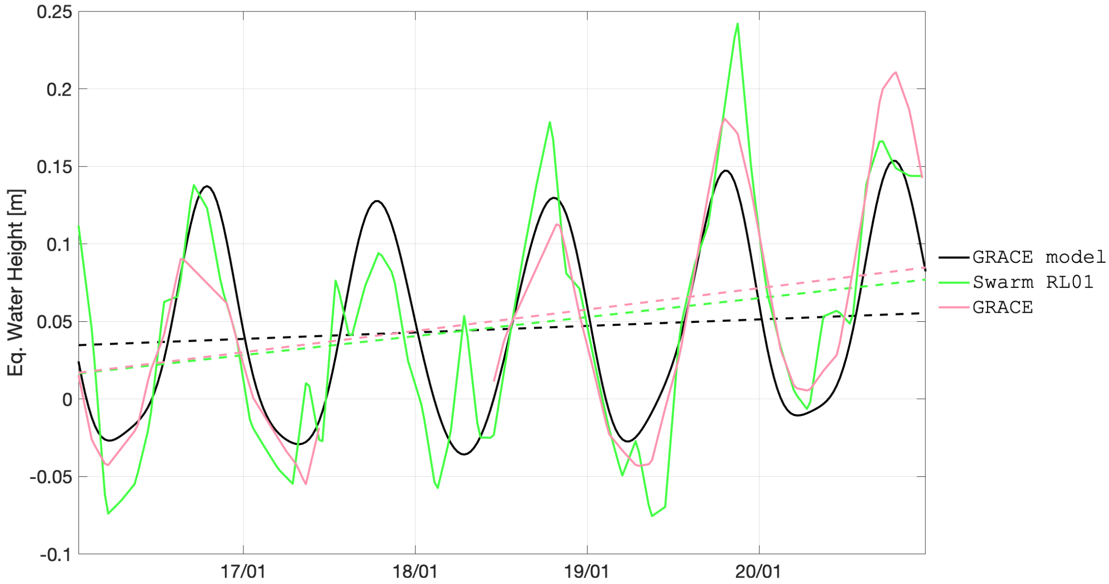

Figure 21 – Time series of EWH for the Eastern Sub-Saharan basin (latitude 1 to 13 degrees, longitude -8 to 35 degrees).

solution	constant term [cm]	constant term Δ [cm]	linear term [cm/year]	linear term Δ [cm/year]	corr. coeff. [ ]
GRACE MODEL	4.50	0.00	0.42	0.00	1.00
Swarm RL01	4.64	0.14	1.23	0.81	0.87
GRACE	4.77	0.27	1.38	0.96	0.92

Table 12 – Statistics of the agreement between GRACE/GRACE-FO and Swarm time series relative to the GRACE/GRACE-FO climatological model for the Eastern Sub-Saharan basin.

The use and/or disclosure, etc. of the contents of this document (or any part thereof) is subject to the restrictions referenced on the front page.

5.4.11 Congo and Zambezi basins

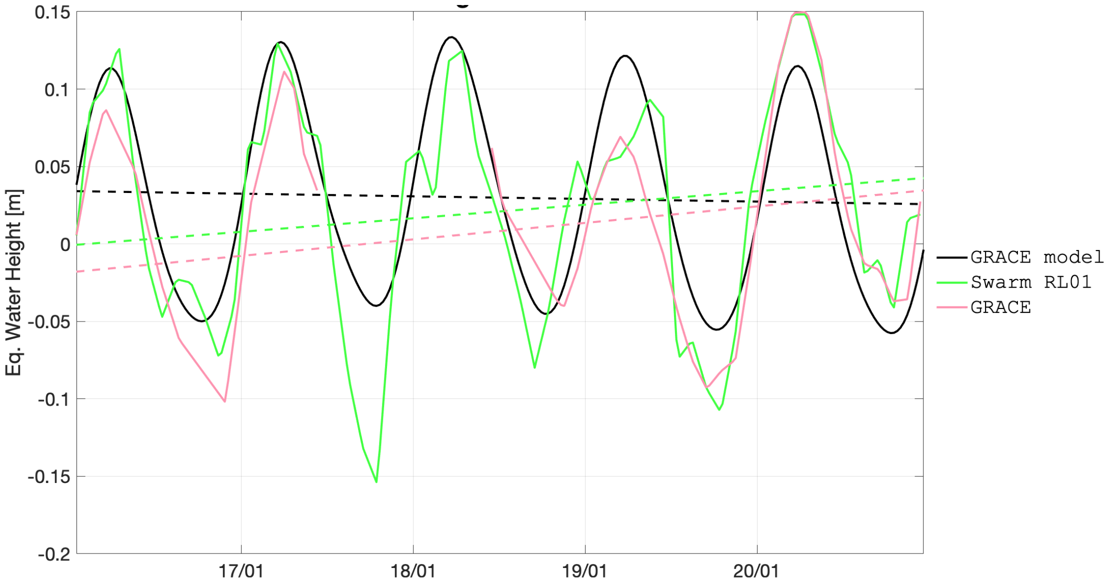

Figure 22 – Time series of EWH for the Congo and Zambezi basins (latitude -23 to -3 degrees, longitude 14 to 38 degrees).

solution	constant term [cm]	constant term Δ [cm]	linear term [cm/year]	linear term Δ [cm/year]	corr. coeff. [ ]
GRACE MODEL	2.99	0.00	-0.17	0.00	1.00
Swarm RL01	2.13	-0.86	0.87	1.04	0.86
GRACE	1.67	-1.32	1.06	1.23	0.87

Table 13 – Statistics of the agreement between GRACE/GRACE-FO and Swarm time series relative to the GRACE/GRACE-FO climatological model for the Congo and Zambezi basins.

5.4.12 Volga basin

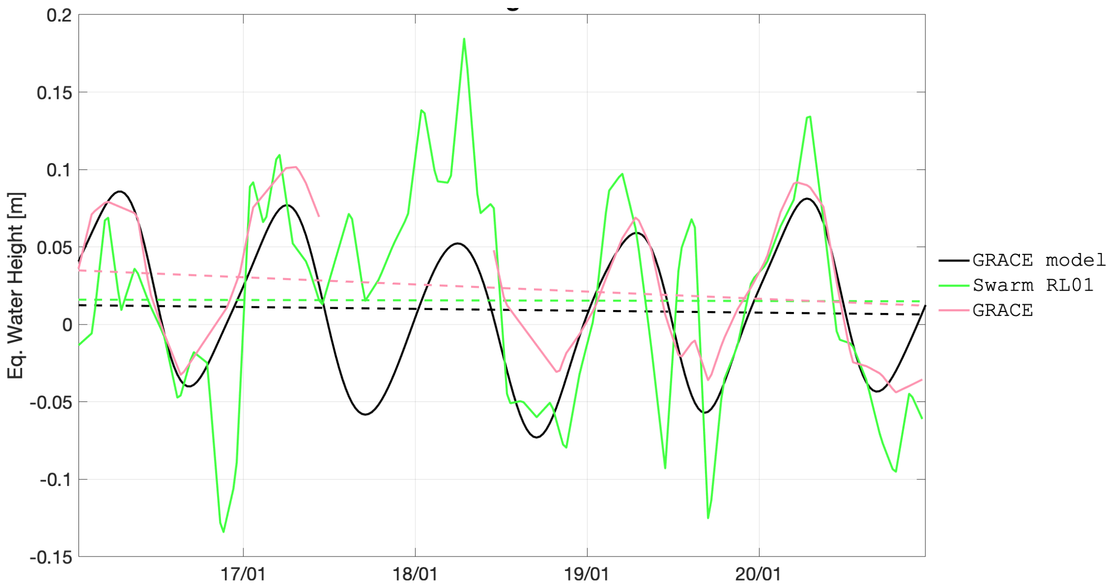

Figure 23 – Time series of EWH for the Volga basin (latitude 53 to 61 degrees, longitude 34 to 56 degrees).

solution	constant term [cm]	constant term Δ [cm]	linear term [cm/year]	linear term Δ [cm/year]	corr. coeff. [ ]
GRACE MODEL	0.94	0.00	-0.12	0.00	1.00
Swarm RL01	1.58	0.63	-0.02	0.10	0.58
GRACE	2.57	1.62	-0.46	-0.34	0.91

Table 14 – Statistics of the agreement between GRACE/GRACE-FO and Swarm time series relative to the GRACE/GRACE-FO climatological model for the Volga basin.

The use and/or disclosure, etc. of the contents of this document (or any part thereof) is subject to the restrictions referenced on the front page.

5.4.13 Siberia region

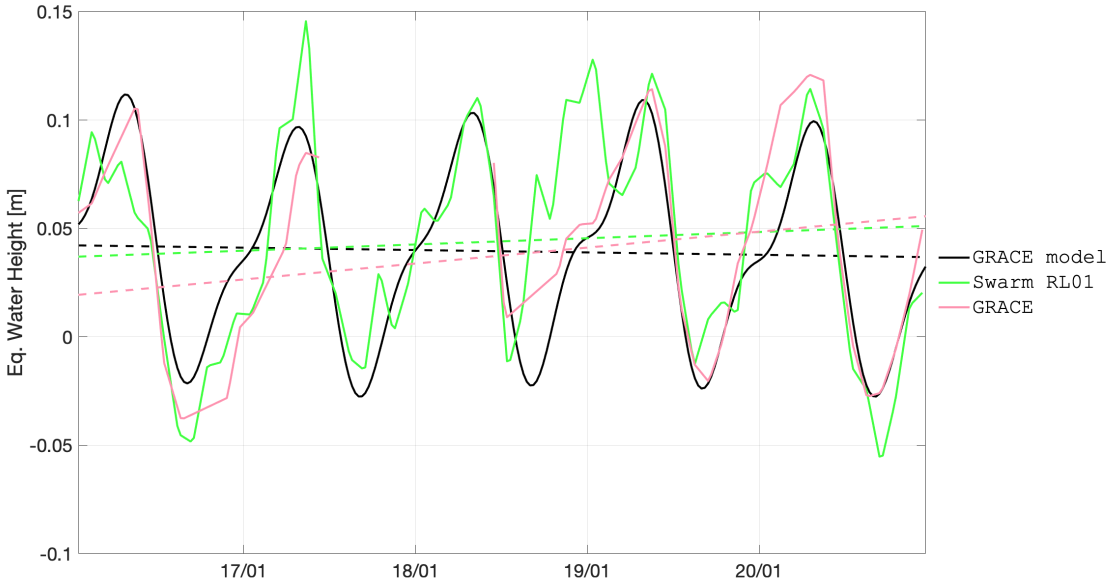

Figure 24 – Time series of EWH for the Siberia region (latitude 57 to 72 degrees, longitude 68 to 109 degrees).

solution	constant term [cm]	constant term Δ [cm]	linear term [cm/year]	linear term Δ [cm/year]	corr. coeff. [ ]
GRACE MODEL	3.95	0.00	-0.11	0.00	1.00
Swarm RL01	4.42	0.47	0.29	0.40	0.80
GRACE	4.59	0.64	0.74	0.84	0.88

Table 15 – Statistics of the agreement between GRACE/GRACE-FO and Swarm time series relative to the GRACE/GRACE-FO climatological model for the Siberia region.

The use and/or disclosure, etc. of the contents of this document (or any part thereof) is subject to the restrictions referenced on the front page.

5.4.14 Ganges-Brahmaputra basin

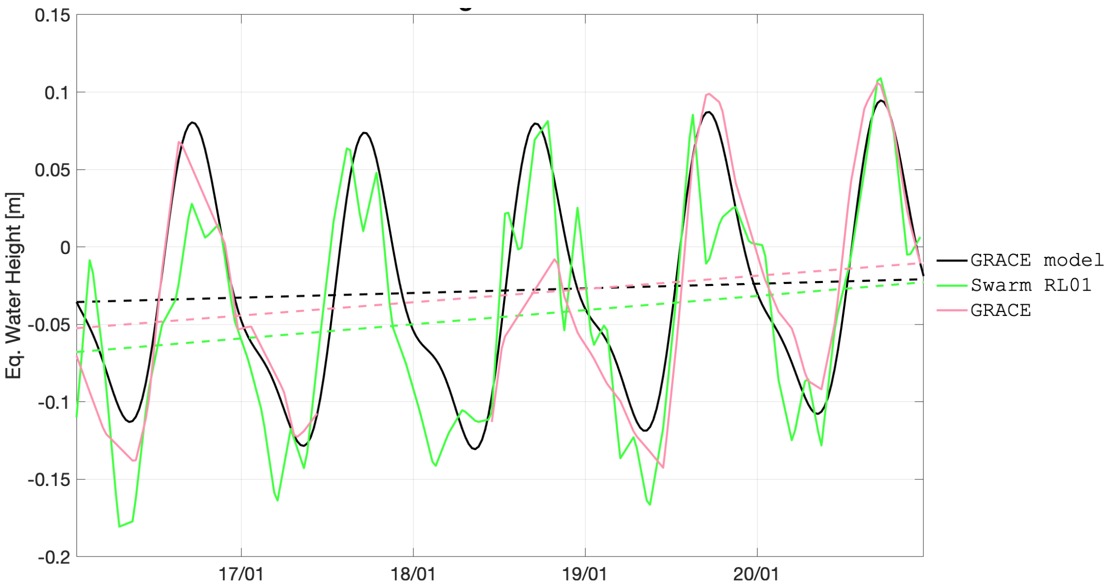

Figure 25 – Time series of EWH for the Ganges-Brahmaputra basin (latitude 15 to 30 degrees, longitude 72 to 89 degrees).

solution	constant term [cm]	constant term Δ [cm]	linear term [cm/year]	linear term Δ [cm/year]	corr. coeff. [ ]
GRACE MODEL	-2.82	0.00	0.30	0.00	1.00
Swarm RL01	-4.56	-1.74	0.92	0.62	0.89
GRACE	-3.98	-1.16	0.86	0.56	0.90

Table 16 – Statistics of the agreement between GRACE/GRACE-FO and Swarm time series relative to the GRACE/GRACE-FO climatological model for the Ganges-Brahmaputra basin.

The use and/or disclosure, etc. of the contents of this document (or any part thereof) is subject to the restrictions referenced on the front page.

5.4.15 Indochina region

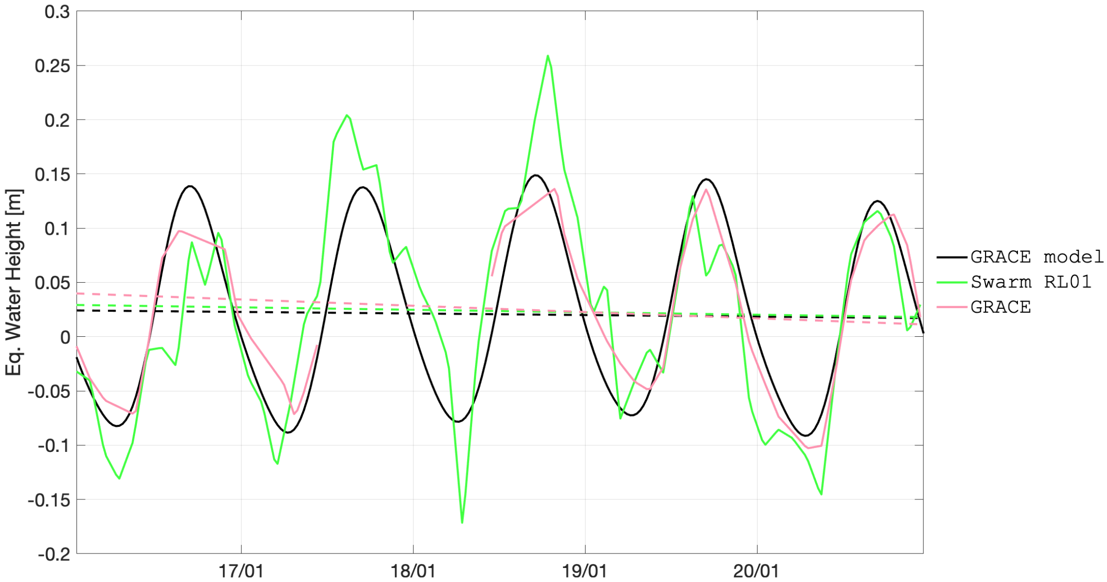

Figure 26 – Time series of EWH for the Indochina region (latitude 12 to 29 degrees, longitude 93 to 105 degrees).

solution	constant term [cm]	constant term Δ [cm]	linear term [cm/year]	linear term Δ [cm/year]	corr. coeff. [ ]
GRACE MODEL	2.07	0.00	-0.14	0.00	1.00
Swarm RL01	2.32	0.26	-0.23	-0.08	0.83
GRACE	1.55	-0.52	-0.58	-0.44	0.96

Table 17 – Statistics of the agreement between GRACE/GRACE-FO and Swarm time series relative to the GRACE/GRACE-FO climatological model for the Indochina region.

5.4.16 Northern Australia region

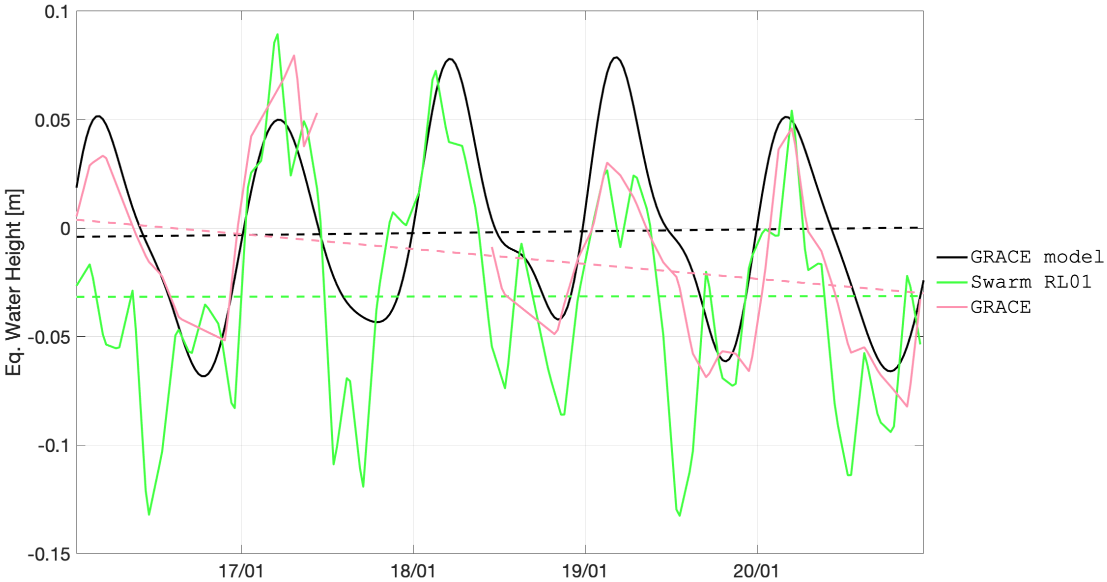

Figure 27 – Time series of EWH for the Northern Australia region (latitude -24 to -10 degrees, longitude 124 to 145 degrees).

solution	constant term [cm]	constant term Δ [cm]	linear term [cm/year]	linear term Δ [cm/year]	corr. coeff. [ ]
GRACE MODEL	-0.19	0.00	0.09	0.00	1.00
Swarm RL01	-3.12	-2.93	0.01	-0.08	0.67
GRACE	-1.26	-1.08	-0.69	-0.77	0.87

Table 18 – Statistics of the agreement between GRACE/GRACE-FO and Swarm time series relative to the GRACE/GRACE-FO climatological model for the Northern Australia region.

The use and/or disclosure, etc. of the contents of this document (or any part thereof) is subject to the restrictions referenced on the front page.

5.4.17 Western Antarctica region

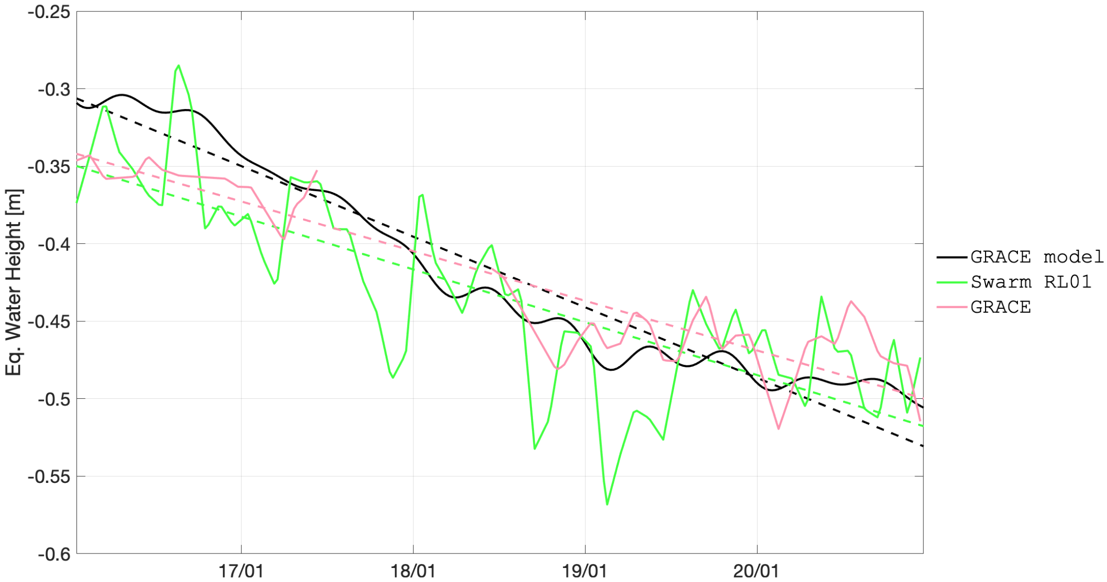

Figure 28 – Time series of EWH for the Western Antarctica region (latitude -80 to -70 degrees, longitude -140 to -85 degrees).

solution	constant term [cm]	constant term Δ [cm]	linear term [cm/year]	linear term Δ [cm/year]	corr. coeff. [ ]
GRACE MODEL	-41.84	0.00	-4.56	0.00	1.00
Swarm RL01	-43.36	-1.53	-3.41	1.15	0.86
GRACE	-43.06	-1.23	-3.20	1.35	0.96

Table 19 – Statistics of the agreement between GRACE/GRACE-FO and Swarm time series relative to the GRACE/GRACE-FO climatological model for the Western Antarctica region.

The use and/or disclosure, etc. of the contents of this document (or any part thereof) is subject to the restrictions referenced on the front page.

5.4.18 Eastern Antarctica region

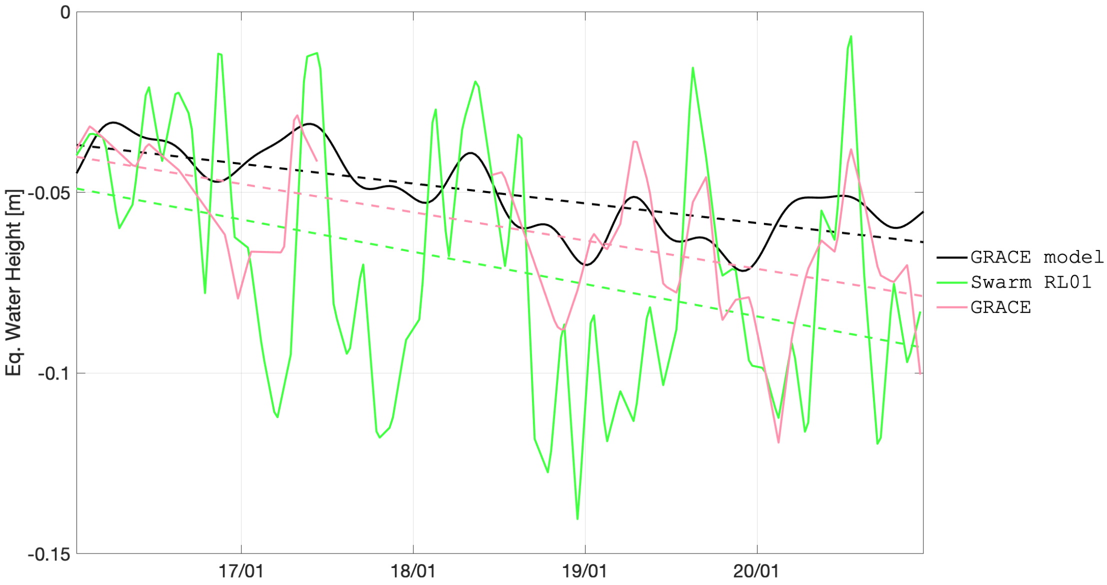

Figure 29 – Time series of EWH for the Eastern Antarctica region (latitude -80 to -68 degrees, longitude 80 to 130 degrees).

solution	constant term [cm]	constant term Δ [cm]	linear term [cm/year]	linear term Δ [cm/year]	corr. coeff. [ ]
GRACE MODEL	-5.03	0.00	-0.55	0.00	1.00
Swarm RL01	-7.10	-2.07	-0.89	-0.35	0.48
GRACE	-6.21	-1.18	-0.78	-0.24	0.64

Table 20 – Statistics of the agreement between GRACE/GRACE-FO and Swarm time series relative to the GRACE/GRACE-FO climatological model for the Eastern Antarctica region.

The use and/or disclosure, etc. of the contents of this document (or any part thereof) is subject to the restrictions referenced on the front page.

5.4.19 Overview

solution	constant term Δ RMS [cm]	linear term Δ RMS [cm/year]	corr. coeff. mean [ ]
GRACE model	0.00	0.00	1.00
Swarm RL01	1.54	0.81	0.76
GRACE	1.12	0.89	0.87

Table 21 – Statistics of the agreement between the GRACE and Swarm time series for the regions displayed in Sections 5.4.1 to 5.4.18.

5.5 Temporal variability

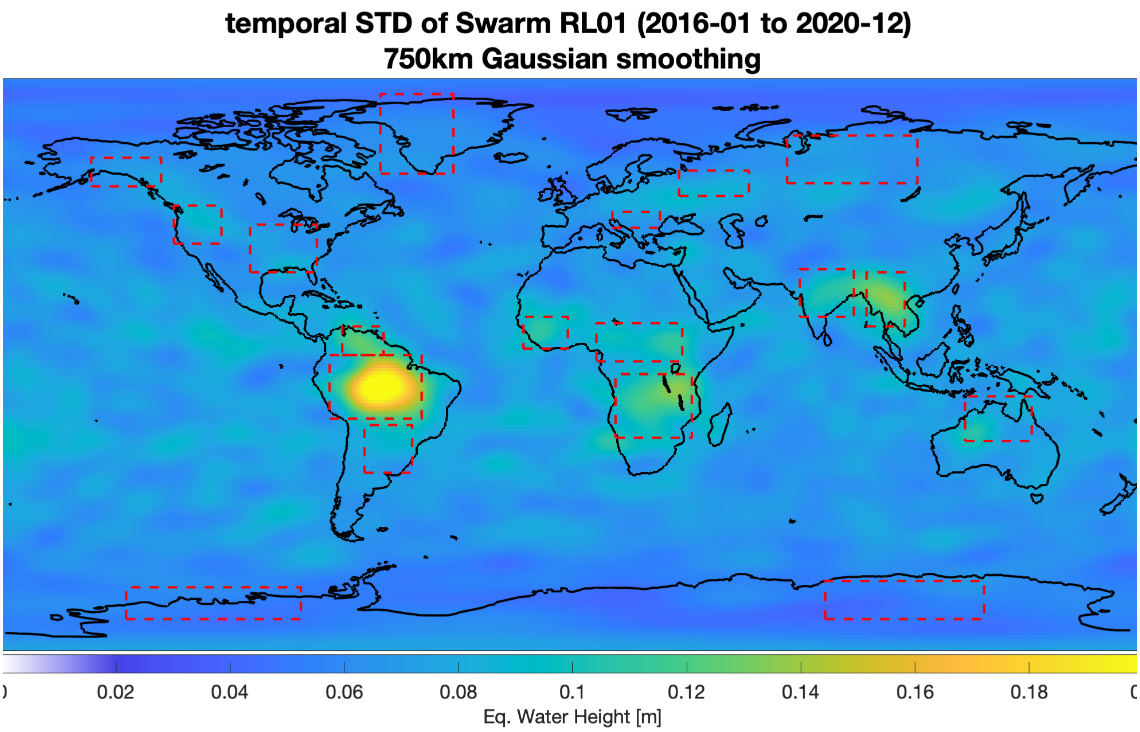

Figure 30 – Temporal variability of the Swarm combined solutions

5.6 Monthly models

Acronyms

AA Acceleration Approach, Rummel (1979)

AIUB Astronomical Institute of the University of Bern, Switzerland, `www.aiub.unibe.ch`

ASU Astronomical Institute (Astronomický ústav), AVCR, Ondřejov, `www.asu.cas.cz/en`

AVCR Czech Academy of Sciences (Akademie věd České Republiky), Czech Republic, `www.avcr.cz/en/`

The use and/or disclosure, etc. of the contents of this document (or any part thereof) is subject to the restrictions referenced on the front page.

CMA	Celestial Mechanics Approach, Beutler et al. (2010)
CSR	Center for Space Research, UT Austin, USA, `www.csr.utexas.edu`
DAA	Decorrelated Acceleration Approach, Bezděk et al. (2014) and Bezděk et al. (2016)
EBA	Energy Balance Approach, O'Keefe (1957) and Jekeli (1999)
EWH	Equivalent Water Height
GFM	Gravity Field Model
GOCE	Gravity field and steady-state Ocean Circulation Explorer, Balmino et al. (1999) and Floberghagen et al. (2011)
GRACE	Gravity Recovery And Climate Experiment, Tapley, Reigber and Melbourne (1996) and Tapley (2004)
GRACE-FO	GRACE Follow On, Kornfeld et al. (2019)
GSFC	Goddard Space Flight Center, United States of America (USA), `www.nasa.gov/centers/goddard`
IEBA	Improved Energy Balance Approach, Shang et al. (2015)
IfG	Institute of Geodesy, TUG, Graz, `www.ifg.tugraz.at`
KO	Kinematic Orbit
N/A	Not Applicable
NEQ	Normal Equation
OSU	Ohio State University, `www.osu.edu`
RL06	Release 6
RMS	Root Mean Squared
SAA	Short-Arcs Approach, Mayer-Gürr (2006)
SH	Spherical Harmonic
SLR	Satellite Laser Ranging, Smith and Turcotte (1993) and Combrinck (2010)
TU Delft	Delft University of Technology, Netherlands, `www.tudelft.nl`
TUG	Graz University of Technology, Austria, `www.tugraz.at`
UT Austin	University of Texas at Austin, `www.utexas.edu`
USA	United States of America
VCE	Variance Component Estimation
WP	Work Package

Symbols

C Stokes coefficient.

References

Balmino, G. et al. (1999). **The Four Candidate Earth Explorer Core Missions - Gravity Field and Steady-State Ocean Circulation Mission**. Tech. rep. SP- 1233(1). Noordwijk, The Netherlands: European Space Agency (cit. on p. 36).

Bettadpur, Srinivas et al. (2015). **Evaluation of the GGM05 Mean Earth Gravity Model**. In: *EGU General Assembly Conference Abstracts* 17, p. 4153 (cit. on p. 6).

Beutler, Gerhard et al. (2010). **The celestial mechanics approach: theoretical foundations**. In: *Journal of Geodesy* 84.10, pp. 605–624. DOI: `10.1007/s00190-010-0401-7` (cit. on pp. 6, 36).

The use and/or disclosure, etc. of the contents of this document (or any part thereof) is subject to the restrictions referenced on the front page.

Bezděk, Aleš et al. (2014). **Gravity field models from kinematic orbits of CHAMP, GRACE and GOCE satellites**. In: *Advances in Space Research* 53.3, pp. 412–429. DOI: 10.1016/j.asr.2013.11.031 (cit. on pp. 6, 36).

Bezděk, Aleš et al. (2016). **Time-variable gravity fields derived from GPS tracking of Swarm**. In: *Geophysical Journal International* 205.3, pp. 1665–1669. DOI: 10.1093/gji/ggw094 (cit. on pp. 6, 36).

Cheng, M. and John Ries (2018). **GRACE Technical Note 11: Monthly estimates of C20 from 5 satellites based on GRACE RL06 models**. Austin, USA. URL: https://podaac-tools.jpl.nasa.gov/drive/files/allData/grace/docs/TN-11_C20_SLR.txt (cit. on p. 7).

Combrinck, Ludwig (2010). **Satellite Laser Ranging**. In: *Sciences of Geodesy - I*. Ed. by Guochang Xu. Berlin, Heidelberg: Springer Berlin Heidelberg. Chap. 9, pp. 301–338. DOI: 10.1007/978-3-642-11741-1_9 (cit. on p. 36).

Floberghagen, Rune et al. (2011). **Mission design, operation and exploitation of the gravity field and steady-state ocean circulation explorer mission**. In: *Journal of Geodesy* 85.11, pp. 749–758. DOI: 10.1007/s00190-011-0498-3 (cit. on p. 36).

Guo, J. Y., X. J. Duan and C. K. Shum (2010). **Non-isotropic Gaussian smoothing and leakage reduction for determining mass changes over land and ocean using GRACE data**. In: *Geophysical Journal International* 181.1, pp. 290–302. DOI: 10.1111/j.1365-246X.2010.04534.x (cit. on p. 7).

Guo, J. Y. et al. (2015). **On the energy integral formulation of gravitational potential differences from satellite-to-satellite tracking**. In: *Celestial Mechanics and Dynamical Astronomy* 121.4, pp. 415–429. DOI: 10.1007/s10569-015-9610-y (cit. on p. 6).

Jäggi, A. et al. (2016). **Swarm kinematic orbits and gravity fields from 18 months of GPS data**. In: *Advances in Space Research* 57.1, pp. 218–233. DOI: 10.1016/j.asr.2015.10.035 (cit. on p. 6).

Jekeli, Christopher (1999). **The determination of gravitational potential differences from satellite-to-satellite tracking**. In: *Celestial Mechanics and Dynamical Astronomy* 75.2, pp. 85–101. DOI: 10.1023/A:1008313405488 (cit. on p. 36).

Kornfeld, Richard P. et al. (2019). **GRACE-FO: The Gravity Recovery and Climate Experiment Follow-On Mission**. In: *Journal of Spacecraft and Rockets* 56.3, pp. 931–951. DOI: 10.2514/1.A34326 (cit. on p. 36).

Loomis, B. D., K. E. Rachlin and S. B. Luthcke (2019). **Improved Earth Oblateness Rate Reveals Increased Ice Sheet Losses and Mass-Driven Sea Level Rise**. In: *Geophysical Research Letters* 46.12, pp. 6910–6917. DOI: 10.1029/2019GL082929 (cit. on pp. 6, 7).

Loomis, B.D. and K.E. Rachlin (2020). **GRACE Technical Note 14: NASA GSFC SLR C20 and C30 solutions**. Greenbelt, USA. URL: https://podaac-tools.jpl.nasa.gov/drive/files/allData/gracefo/docs/TN-14_C30_C20_GSFC_SLR.txt (cit. on p. 7).

Mayer-Gürr, Torsten (2006). **Gravitationsfeldbestimmung aus der Analyse kurzer Bahnbögen am Beispiel der Satellitenmissionen CHAMP und GRACE**. PhD thesis. Rheinischen Friedrich-Wilhelms Universität Bonn. URL: http://hss.ulb.uni-bonn.de/2006/0904/0904.pdf (cit. on pp. 6, 36).

O'Keefe, John A. (1957). **An application of Jacobi's integral to the motion of an earth satellite**. In: *The Astronomical Journal* 62, p. 265. DOI: 10.1086/107530 (cit. on p. 36).

Rummel, R. (1979). **Determination of short-wavelength components of the gravity field from satellite-to-satellite tracking or satellite gradiometry**. In: *Manuscripta Geodaetica* 4.2, pp. 107–148 (cit. on p. 35).

The use and/or disclosure, etc. of the contents of this document (or any part thereof) is subject to the restrictions referenced on the front page.

Shang, Kun et al. (2015). **GRACE time-variable gravity field recovery using an improved energy balance approach**. In: *Geophysical Journal International* 203.3, pp. 1773–1786. DOI: `10.1093/gji/ggv392` (cit. on pp. 6, 36).

Smith, David E. and Donald L. Turcotte (1993). **Millimeter Accuracy Satellite Laser Ranging: a Review**. In: *Contributions of Space Geodesy to Geodynamics: Technology*. Ed. by John J. Degnan. Vol. 25. Geodynamics Series. Washington, D. C.: American Geophysical Union. DOI: `10.1029/GD025p0133` (cit. on p. 36).

Tapley, B., C. Reigber and W Melbourne (1996). **Gravity Recovery And Climate Experiment (GRACE) mission**. Baltimore, USA (cit. on p. 36).

Tapley, Byron D. (2004). **GRACE Measurements of Mass Variability in the Earth System**. In: *Science* 305.5683, pp. 503–505. DOI: `10.1126/science.1099192` (cit. on p. 36).

Teixeira da Encarnação, João and Pieter Visser (2017). **TN-01 : Standards and Background Models**. Tech. rep. Delft, the Netherlands: Delft University of Technology. DOI: `10.13140/RG.2.2.12840.32006/1` (cit. on p. 5).

— (2019). **TN-03: Swarm models validation**. Tech. rep. TU Delft. DOI: `10.13140/RG.2.2.33313.76640` (cit. on pp. 5, 6).

Zehentner, Norbert and Torsten Mayer-Gürr (2016). **Precise orbit determination based on raw GPS measurements**. In: *Journal of Geodesy* 90.3, pp. 275–286. DOI: `10.1007/s00190-015-0872-7` (cit. on p. 6).

The use and/or disclosure, etc. of the contents of this document (or any part thereof) is subject to the restrictions referenced on the front page.